Article

Microbial bile acid metabolites modulate gut RORγ$^+$ regulatory T cell homeostasis

https://doi.org/10.1038/s41586-019-1865-0

Received: 15 March 2019

Accepted: 7 November 2019

Published online: 25 December 2019

Xinyang Song[1,5], Ximei Sun[1,5], Sungwhan F. Oh[1,2], Meng Wu[1], Yanbo Zhang[1], Wen Zheng[1], Naama Geva-Zatorsky[1,4], Ray Jupp[3], Diane Mathis[1], Christophe Benoist[1] & Dennis L. Kasper[1]*

The metabolic pathways encoded by the human gut microbiome constantly interact with host gene products through numerous bioactive molecules[1]. Primary bile acids (BAs) are synthesized within hepatocytes and released into the duodenum to facilitate absorption of lipids or fat-soluble vitamins[2]. Some BAs (approximately 5%) escape into the colon, where gut commensal bacteria convert them into various intestinal BAs[2] that are important hormones that regulate host cholesterol metabolism and energy balance via several nuclear receptors and/or G-protein-coupled receptors[3,4]. These receptors have pivotal roles in shaping host innate immune responses[1,5]. However, the effect of this host–microorganism biliary network on the adaptive immune system remains poorly characterized. Here we report that both dietary and microbial factors influence the composition of the gut BA pool and modulate an important population of colonic FOXP3$^+$ regulatory T (T_{reg}) cells expressing the transcription factor RORγ. Genetic abolition of BA metabolic pathways in individual gut symbionts significantly decreases this T_{reg} cell population. Restoration of the intestinal BA pool increases colonic RORγ$^+$ T_{reg} cell counts and ameliorates host susceptibility to inflammatory colitis via BA nuclear receptors. Thus, a pan-genomic biliary network interaction between hosts and their bacterial symbionts can control host immunological homeostasis via the resulting metabolites.

FOXP3$^+$ T_{reg} cells residing in the gut lamina propria are critical in regulating intestinal inflammation[6,7]. A distinct T_{reg} cell population expressing the transcription factor RORγ is induced in the colonic lamina propria by colonization with gut symbionts[8–13]. Unlike thymic T_{reg} cells, colonic RORγ$^+$ T_{reg} cells have a distinct phenotype (Helios$^-$ and NRP1$^-$), and their accumulation is influenced by enteric factors derived from diet or commensal colonization[8,9]. We hypothesized that intestinal bacteria facilitate the induction of RORγ$^+$ T_{reg} cells by modifying metabolites resulting from the host's diet, and analysed RORγ$^+$Helios$^-$ cells in the colonic T_{reg} cell population from specific pathogen-free (SPF) mice fed different diets—that is, a nutrient-rich diet or a minimal diet (Supplementary Table 1). We compared RORγ$^+$ T_{reg} cells in these groups with those in germ-free (GF) mice fed a nutrient-rich diet (Fig. 1a). Both minimal-diet SPF mice and rich-diet GF mice had a lower number of RORγ$^+$Helios$^-$ cells in the colonic T_{reg} cell population than did rich-diet SPF mice (Fig. 1a and Extended Data Fig. 1a). The effect of diet on T_{reg} cell homeostatic proportions was limited to the colon and was not observed in other regions of the intestinal tract (the duodenum, jejunum or ileum) or in other lymphoid organs (the thymus, spleen, lymph nodes or Peyer's patches) (Extended Data Fig. 1b, c). When diets were switched from minimal to nutrient-rich, colonic RORγ$^+$ T_{reg} cell frequency was reversed (Extended Data Fig. 1d–f). This finding suggested that dietary components or their resulting products biotransformed by the host and its bacterial symbionts are probably responsible for the induction of colonic RORγ$^+$ T_{reg} cells. Consistent with our previous findings[8], we determined that, in our mouse colony, short-chain fatty acids (SCFAs) alone appear to be irrelevant to the accumulation of colonic RORγ$^+$ T_{reg} cells (Extended Data Fig. 1g–j).

As intestinal BAs are important metabolites affected by the host's diet and modified by gut bacteria, we checked the intestinal BA contents of these mice (Supplementary Table 2). The level of murine conjugated primary BAs (the taurine-conjugated species of cholic acid, chenodeoxycholic acid, muricholic acids and ursodeoxycholic acid (TCA, TCDCA, TMCAs and TUDCA, respectively)[14]) was greatly reduced in the faeces of minimal-diet SPF mice (Fig. 1b). Not surprisingly, the GF mice had accumulated conjugated primary BAs (Fig. 1b). However, along with the reduced RORγ$^+$ T_{reg} cell population, the levels of faecal deconjugated primary BAs and secondary BAs were significantly lower in both minimal-diet SPF mice and rich-diet GF mice than in rich-diet SPF mice (Fig. 1c, d). These results suggested that host BAs generated in response to diet and biotransformed by bacteria may induce colonic RORγ$^+$ T_{reg} cells.

To directly test whether BA metabolites regulate colonic RORγ$^+$ T_{reg} cells, we supplemented the drinking water of minimal-diet SPF mice with either individual or combinations of BAs (Fig. 1e). Neither individual primary nor secondary BAs rescued the counts of colonic RORγ$^+$ T_{reg} cells or total FOXP3$^+$ T_{reg} cells. However, mixtures of certain murine primary BAs (cholic/ursodeoxycholic acids,

[1]Department of Immunology, Blavatnik Institute, Harvard Medical School, Boston, MA, USA. [2]Center for Experimental Therapeutics and Reperfusion Injury, Department of Anesthesiology, Perioperative and Pain Medicine, Brigham and Women's Hospital, Harvard Medical School, Boston, MA, USA. [3]UCB Pharma, Slough, UK. [4]Present address: Department of Cell Biology and Cancer Science, Rappaport Faculty of Medicine, Technion Integrated Cancer Center, Technion–Israel Institute of Technology, Haifa, Israel. [5]These authors contributed equally: Xinyang Song, Ximei Sun. *e-mail: dennis_kasper@hms.harvard.edu

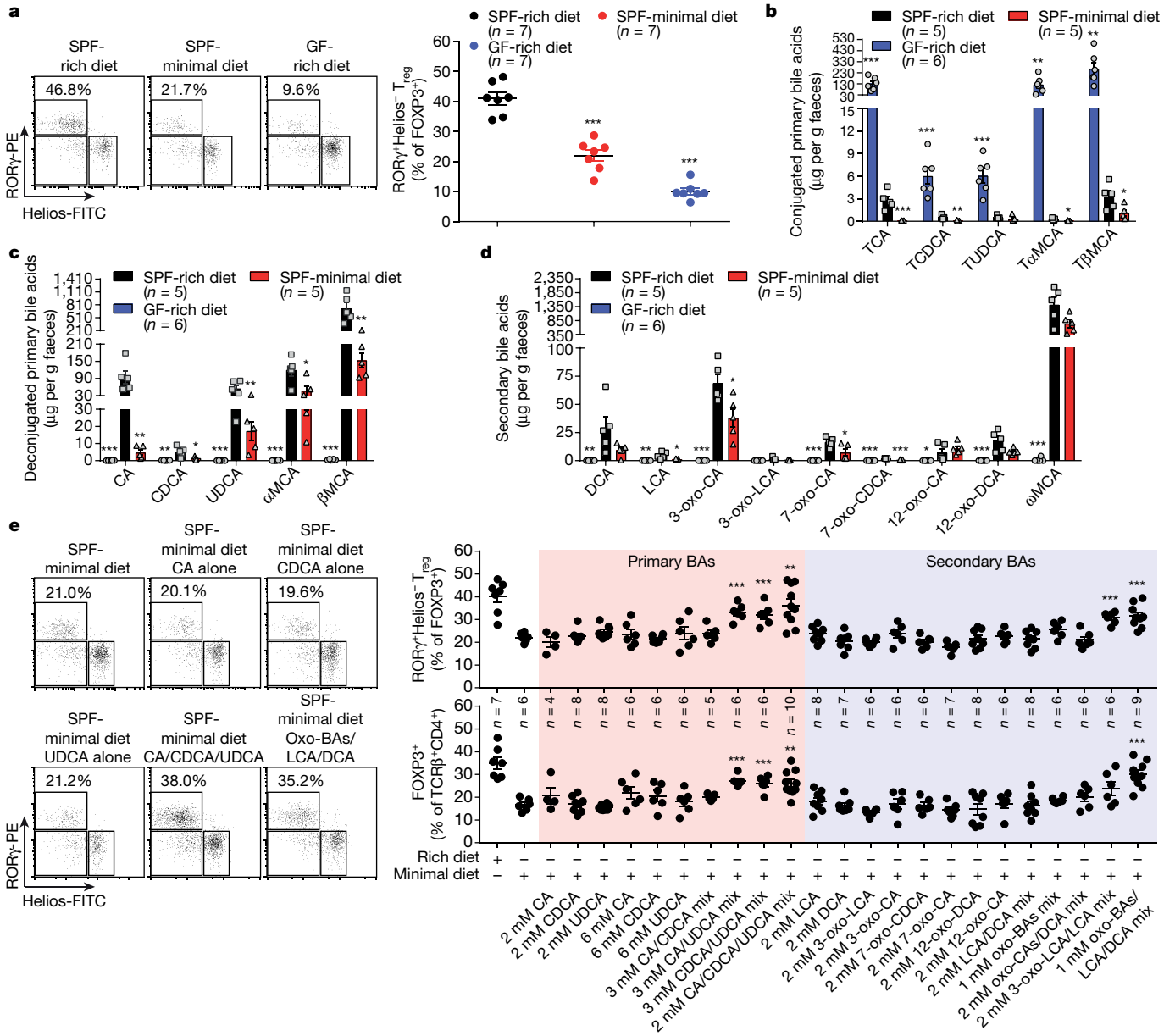

Fig. 1 | Gut BA metabolites are essential for colonic RORγ$^+$ T$_{reg}$ cell maintenance. a, Beginning at 3 weeks of age, three groups of mice were fed special diets for 4 weeks. SPF mice were fed either a nutrient-rich or a minimal diet, and GF mice were fed the nutrient-rich diet. Representative plots and frequencies of RORγ$^+$Helios$^-$ in the FOXP3$^+$CD4$^+$TCRβ$^+$ T$_{reg}$ cell population are shown. **b**–**d**, Liquid chromatography–mass spectrometry (LC–MS) quantification of faecal conjugated primary BAs (**b**), deconjugated primary BAs (**c**) and secondary BAs (**d**) from groups of mice fed as in **a**. The BAs determined were cholic acid (CA), chenodeoxycholic acid (CDCA), ursodeoxycholic acid (UDCA), α-muricholic acid (αMCA), βMCA, deoxycholic acid (DCA), lithocholic acid (LCA), 3-oxo-CA, 3-oxo-LCA, 7-oxo-CA, 7-oxo-CDCA, 12-oxo-CA, 12-oxo-DCA, ωMCA and taurine-conjugated species (TCA, TCDCA, TUDCA, TαMCA and TβMCA). **e**, Three-week-old SPF mice were fed a nutrient-rich diet, a minimal diet, or a minimal diet supplemented with one or more primary or secondary BAs in drinking water for 4 weeks. Representative plots and frequencies of colonic RORγ$^+$Helios$^-$ in the FOXP3$^+$CD4$^+$TCRβ$^+$ T$_{reg}$ cell population and of colonic FOXP3$^+$ in the CD4$^+$TCRβ$^+$ cell population are shown. The BAs used in the feed were CA, CDCA, UDCA, DCA, LCA, 3-oxo-CA, 3-oxo-LCA, 7-oxo-CA, 7-oxo-CDCA, 12-oxo-CA, 12-oxo-DCA and various indicated BA combinations. Data are representative of at least two independent experiments in **a**–**d**. Data are pooled from three independent experiments in **e**. *n* represents biologically independent animals. Data are mean ± s.e.m. $^*P < 0.05$, $^{**}P < 0.01$, $^{***}P < 0.001$, one-way analysis of variance (ANOVA) followed by the Bonferroni post hoc test.

chenodeoxycholic/ursodeoxycholic acids or cholic/chenodeoxycholic/ursodeoxycholic acids) restored colonic frequencies of both RORγ$^+$ T$_{reg}$ cells and FOXP3$^+$ T$_{reg}$ cells close to that in rich-diet mice (Fig. 1e and Extended Data Fig. 2a, b). Similarly, a mixture of eight representative secondary BAs from bacterial oxidation and dehydroxylation pathways significantly increased the number of colonic RORγ$^+$ T$_{reg}$ cells and FOXP3$^+$ T$_{reg}$ cells in minimal-diet mice (Fig. 1e and Extended Data Fig. 2a, b). We tested several more combinations of secondary BAs and found that only a combination of lithocholic/3-oxo-lithocholic acids restored colonic RORγ$^+$ T$_{reg}$ counts (Fig. 1e). No similar effect of these BAs was found on colonic type 17 T helper (T$_H$17) cells (Extended Data Fig. 2c), or on RORγ$^+$ T$_{reg}$ cells or T$_H$17 cells from the spleen, mesenteric lymph node or small intestine (Extended Data Fig. 2d, e). These results indicated that certain primary and secondary BA species within a BA pool preferentially regulate RORγ$^+$ T$_{reg}$ cells and that modulation of this T$_{reg}$ cell population by BAs is both cell-type and tissue-type specific.

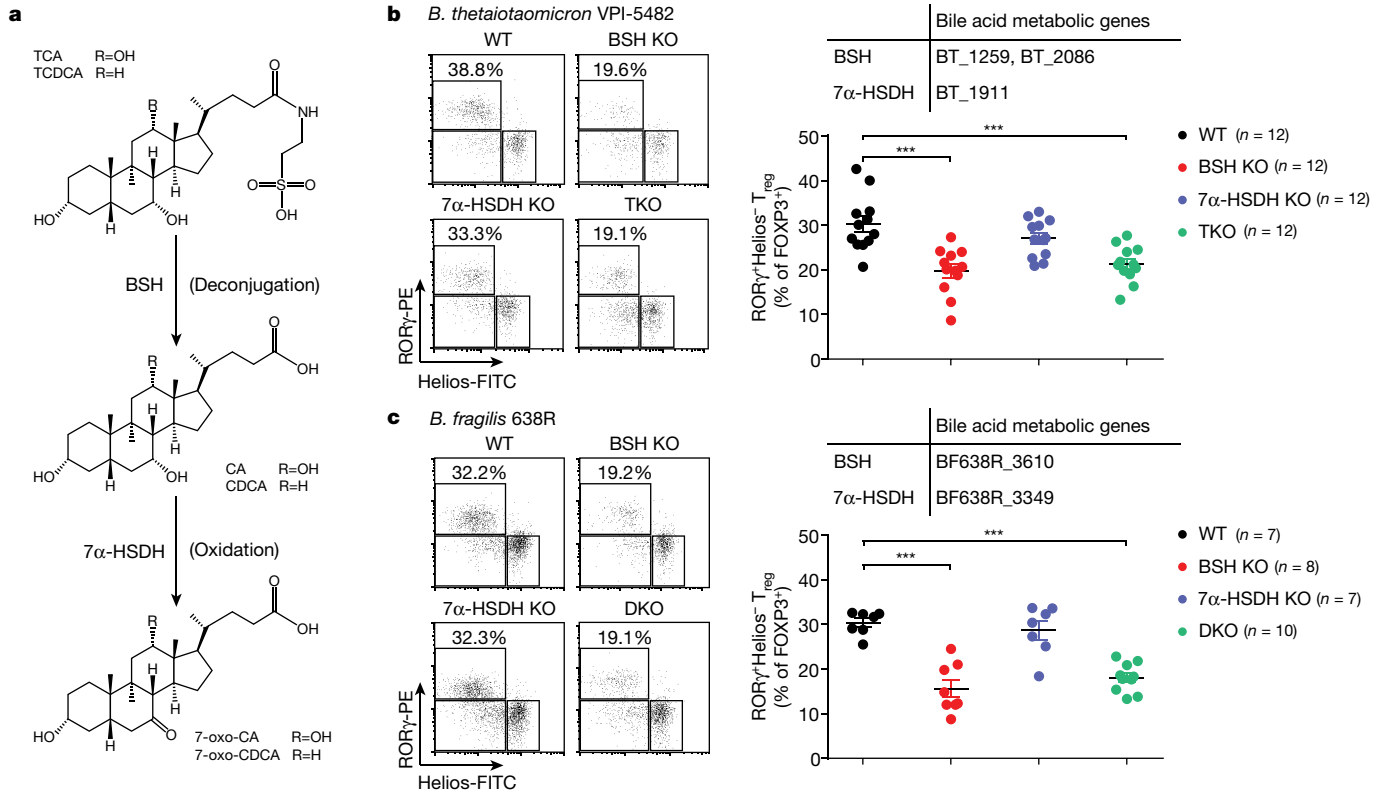

Fig. 2 | Gut bacteria control colonic RORγ$^+$T$_{reg}$ cells through their BA metabolic pathways. a, Schematic diagram of BA metabolic pathways in *B. thetaiotaomicron* and *B. fragilis*. **b**, Each of the four groups of GF mice was colonized with one of the following microorganisms for 2 weeks: (1) a wild-type (WT) strain of *B. thetaiotaomicron*; (2) a BSH-mutant strain (BSH KO, in which both the BT_1259 and BT_2086 genes are deleted); (3) a 7α-HSDH-mutant strain (7α-HSDH KO, in which the BT_1911 gene is deleted); or (4) a triple-mutant strain (TKO; in which all three genes are deleted). Representative plots and frequencies of RORγ$^+$Helios$^-$ in the colonic FOXP3$^+$CD4$^+$TCRβ$^+$T$_{reg}$ cell population are shown. **c**, Each of the four groups of GF mice was colonized with one of the following microorganisms for 2 weeks: (1) a wild-type strain of *B. fragilis*; (2) a BSH-KO strain (in which the BF638R_3610 gene is deleted); (3) a 7α-HSDH-KO strain (in which the BF638R_3349 gene is deleted); or (4) a double-mutant strain (DKO; in which both genes are deleted). Colonic T$_{reg}$ cells were analysed as in **b**. Data are pooled from three independent experiments in **b** and **c**. *n* represents biologically independent animals. Data are mean ± s.e.m. (**b** and **c**). ***$P < 0.001$, one-way ANOVA followed by the Bonferroni post hoc test.

As colonic BAs are derived mainly from bacterial biomodifications[2], we sought to determine how BA-producing bacteria regulate colonic RORγ$^+$T$_{reg}$ cells. Although the composition of the gut microbiota reorganized in minimal-diet mice (Extended Data Fig. 3a–c), BA-metabolizing bacteria—for example, Bacteroidetes and Firmicutes—remained the dominant phyla within the minimal-diet mouse intestine (Extended Data Fig. 3d). Neither dietary alteration nor BA supplementation affected the level of recognized secondary BA-generating bacteria—that is, *Clostridium* cluster IV or XIVα—in the colons of these mice (Extended Data Fig. 3e), which suggests that the decrease in the number of RORγ$^+$T$_{reg}$ cells in minimal-diet mice is not due to the loss of BA-producing bacteria. Minimal-diet GF mice had low numbers of colonic RORγ$^+$T$_{reg}$ cells, as did rich-diet GF mice (Extended Data Fig. 3f). Transferring the gut microbiota from minimal-diet SPF mice into rich-diet GF mice—but not transfer into minimal-diet GF mice—fully restored the frequencies of colonic RORγ$^+$T$_{reg}$ cells (Extended Data Fig. 3f). These results suggested that switching diet alone is insufficient to tune RORγ$^+$T$_{reg}$ cells, while, in response to dietary stimuli, bacteria within the gut modulate this T$_{reg}$ cell population.

Several phyla and genera of human gastrointestinal bacteria can induce RORγ$^+$T$_{reg}$ cells, and these same microorganism can also salvage conjugated BAs escaping from active transport in the ileum and convert them into various BA derivatives[2,15,16]. We hypothesized that BA metabolic pathways in these bacteria are involved in the induction of colonic RORγ$^+$T$_{reg}$ cells. We chose two RORγ$^+$T$_{reg}$ cell inducers—*Bacteroides thetaiotaomicron* and *Bacteroides fragilis*—to test this hypothesis, as they harbour simple BA metabolic pathways and are genetically tractable[17] (Fig. 2a). Using the suicide vector pNJR6 for *Bacteroides*[18], we knocked out the genes that encode proteins involved in both BA deconjugation (bile salt hydrolase (BSH)) and oxidation of hydroxy groups at the C-7 position (7α-hydroxysteroid dehydrogenase (7α-HSDH)) (Extended Data Fig. 4a, b). A genetic deficiency of the BA metabolic genes in these two species did not affect the ability of bacteria to colonize GF mouse colons (Extended Data Fig. 4c, d). Knockout of genes encoding BSH in these species altered the BA pool in monocolonized GF mice and impaired in vivo deconjugation of BAs (Extended Data Fig. 4e, f). These results were consistent with a recent report on the functions of BSH in *Bacteroides*[15]. Notably, we detected no BA level changes after deletion of the genes encoding 7α-HSDH, indicating that in these bacterial species, 7α-oxidation may not have a major role in BA metabolism. Elimination of BSH or the entire BA metabolic pathway in *Bacteroides*—a triple knockout (TKO) in *B. thetaiotaomicron* or a double knockout (DKO) in *B. fragilis*—dampened bacterial ability to induce colonic RORγ$^+$T$_{reg}$ cells (Fig. 2b, c and Extended Data Fig. 5a, c). By contrast, 7α-HSDH mutants elicited counts of colonic RORγ$^+$T$_{reg}$ cells comparable to those induced by wild-type *Bacteroides* (Fig. 2b, c and Extended Data Fig. 5a, c). As *Bacteroides* do not harbour typical biotransformation pathways for secondary BA generation[2], the decrease in the number of RORγ$^+$T$_{reg}$ cells in BSH-mutant-associated GF mice indicated a direct role for primary BAs in regulating this T$_{reg}$ cell population. Deletion of BA biotransformation pathways in *Bacteroides* did not alter the ability of these species to induce colonic total FOXP3$^+$T$_{reg}$ cells, colonic T$_H$17 cells (Extended

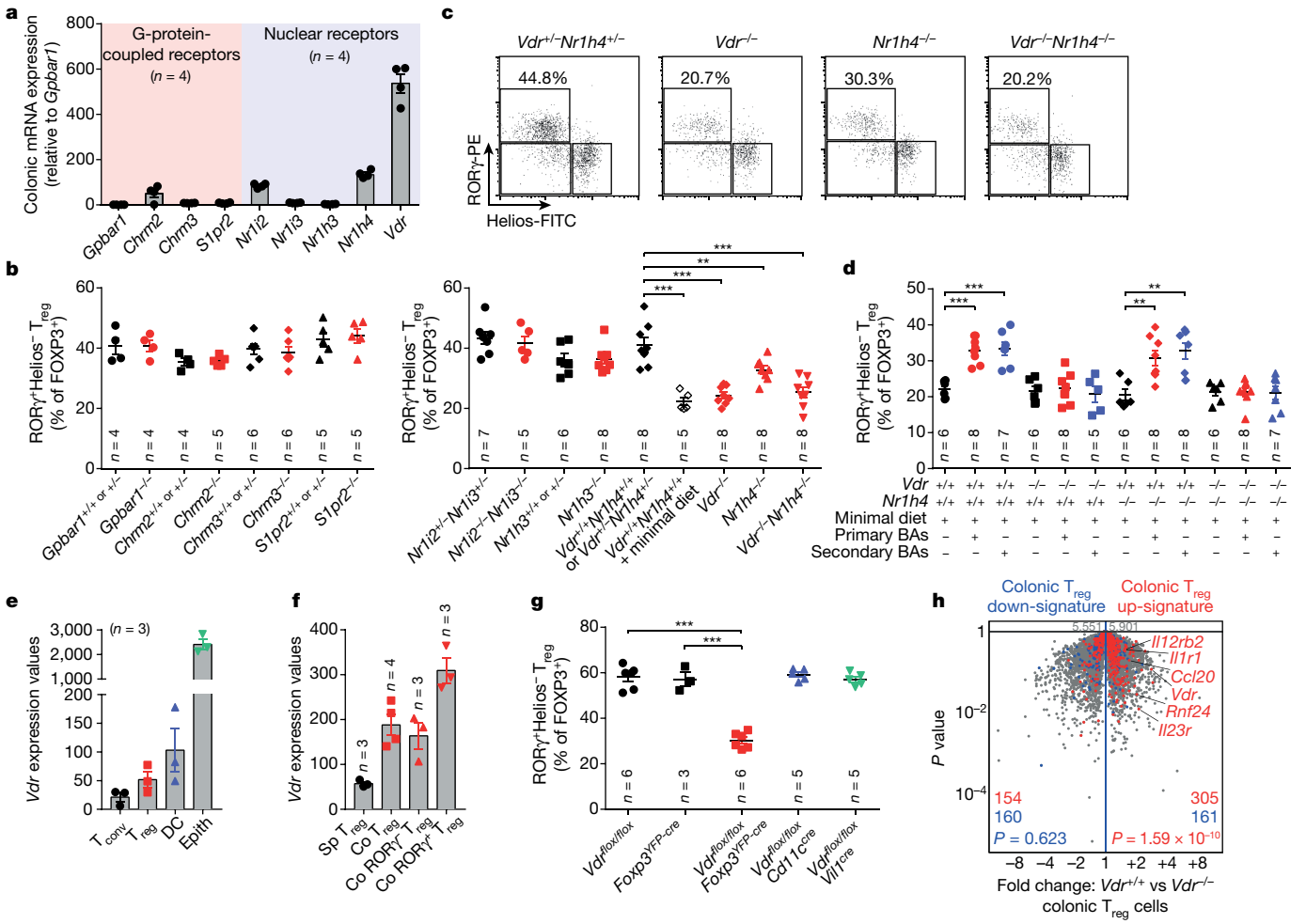

Fig. 3 | BA metabolites modulate colonic RORγ$^+$ T_{reg} cells via BARs. **a**, Quantitative mRNA expression of BARs in the colon of SPF mice. **b**, Frequencies of colonic RORγ$^+$Helios$^-$ in the FOXP3$^+$CD4$^+$TCRβ$^+$ T_{reg} cell population from mice deficient in G-protein-coupled receptors (*Gpbar1*$^{-/-}$, *Chrm2*$^{-/-}$, *Chrm3*$^{-/-}$ and *S1pr2*$^{-/-}$) and their littermate controls. **c**, Representative plots and frequencies of colonic RORγ$^+$Helios$^-$ in the FOXP3$^+$CD4$^+$TCRβ$^+$ T_{reg} cell population from mice deficient in nuclear receptors (*Nr1i2*$^{-/-}$*Nr1i3*$^{-/-}$, *Nr1h3*$^{-/-}$, *Vdr*$^{-/-}$, *Nr1h4*$^{-/-}$ and *Vdr*$^{-/-}$*Nr1h4*$^{-/-}$), their littermate controls and minimal-diet *Vdr*$^{+/+}$*Nr1h4*$^{+/+}$ mice. **d**, Three-week-old *Vdr*$^{+/+}$*Nr1h4*$^{+/+}$, *Vdr*$^{-/-}$, *Nr1h4*$^{-/-}$ and *Vdr*$^{-/-}$*Nr1h4*$^{-/-}$ mice were fed a minimal diet or a minimal diet supplemented with primary BAs (CA/CDCA/UDCA, 2 mM of each) or secondary BAs (DCA/LCA/3-oxo-CA/3-oxo-LCA/7-oxo-CA/7-oxo-CDCA/12-oxo-CA/12-oxo-DCA, 1 mM of each) in their drinking water for 4 weeks. Frequencies of colonic RORγ$^+$Helios$^-$ in the FOXP3$^+$CD4$^+$TCRβ$^+$ T_{reg} cell population are shown. **e**, Normalized expression values of *Vdr* in colonic T_{conv} cells, FOXP3$^+$ T_{reg} cells, dendritic cells (DCs) and epithelial cells (Epith). **f**, Normalized expression values of *Vdr* in splenic T_{reg} cells (Sp T_{reg}), colonic T_{reg} cells (Co T_{reg}), colonic RORγ$^-$ T_{reg} cells (Co RORγ$^-$ T_{reg}) and colonic RORγ$^+$ T_{reg} cells (Co RORγ$^+$ T_{reg}). **g**, Frequencies of colonic RORγ$^+$Helios$^-$ in the FOXP3$^+$CD4$^+$TCRβ$^+$ T_{reg} cell population from *Vdr*$^{flox/flox}$*Foxp3*$^{YFP\text{-}cre}$, *Vdr*$^{flox/flox}$*Cd11c*^{cre} and *Vdr*$^{flox/flox}$*Vil1*^{cre} mice and from *Vdr*$^{flox/flox}$ and *Foxp3*$^{YFP\text{-}cre}$ mice. **h**, Volcano plots comparing transcriptomes of colonic T_{reg} cells from *Vdr*$^{+/+}$*Foxp3*^{mRFP} or *Vdr*$^{-/-}$*Foxp3*^{mRFP} mice ($n = 3$). Colonic T_{reg} cell signature genes are highlighted in red (upregulated) or blue (downregulated). Data are pooled from two or three independent experiments. *n* represents biologically independent animals. Data are mean ± s.e.m. $^{**}P < 0.01$, $^{***}P < 0.001$, one-way ANOVA followed by the Bonferroni post hoc test (**c**, **d** and **g**) or χ^2 test (**h**).

Data Fig. 5b, d–h), or T_{reg} cells and T_H17 cells in the spleen, mesenteric lymph node and small intestine (Extended Data Fig. 5i–l).

Host BAs are metabolically modified by microorganisms and used as signalling molecules, serving as ligands that activate BA receptors (BARs)[4]. Thus, we explored whether BARs modulate gut RORγ$^+$ T_{reg} cell homeostasis. By comparing mouse colonic tissue expression of various BARs, we found that nuclear receptors, especially vitamin D receptor (VDR), were more abundant (Fig. 3a and Extended Data Fig. 6a). Next, we compared the numbers of colonic RORγ$^+$ T_{reg} cells in mice genetically deficient in each of several BARs. G-protein-coupled receptor deficiency did not affect the number of colonic RORγ$^+$ T_{reg} cells (Fig. 3b). The nuclear receptors NR1I2/3 (also known as PXR/CAR) and NR1H3 (also known as LXRα) were also non-contributory (Fig. 3c and Extended Data Fig. 6b). However, deficiency in either of the two BA-sensing nuclear receptors—VDR and NR1H4 (also known as FXR)[19,20]—compromised the number of colonic RORγ$^+$ T_{reg} cells (Fig. 3c and Extended Data Fig. 6b). The colonic RORγ$^+$ T_{reg} cell phenotype of mice with loss of both of these genes resembled that of mice with loss of only *Vdr* or in minimal-diet littermate controls (Fig. 3c and Extended Data Fig. 6b). This result indicated a prominent role for VDR signalling in modulating this colonic T_{reg} cell population. That all BAR-deficient mice had normal colonic counts of total FOXP3$^+$ T_{reg} cells and T_H17 cells (Extended Data Fig. 6c–g) as well as RORγ$^+$ T_{reg} cells in the spleen, mesenteric lymph node and small intestine (Extended Data Fig. 6h–n) indicated that BAR signalling control of RORγ$^+$ T_{reg} cells is tissue dependent.

To determine whether intestinal BAs modulate colonic RORγ$^+$ T_{reg} cells via VDR or NR1H4, we treated nuclear receptor-deficient mice with a mixture of three murine primary BAs (cholic/chenodeoxycholic/ursodeoxycholic acids) or a mixture of eight murine secondary BAs (deoxycholic acid/lithocholic acid/oxidized BAs). Both mixtures of

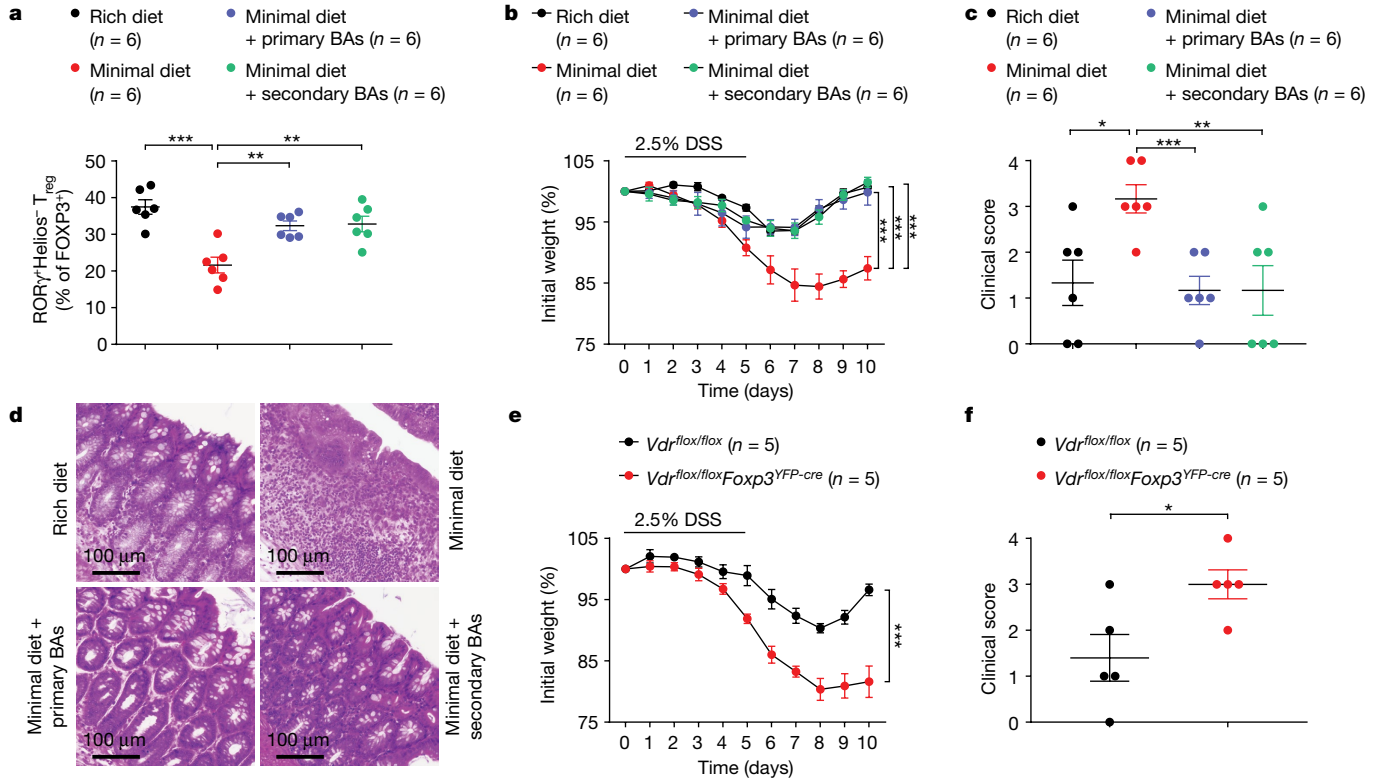

Fig. 4 | BAs ameliorate gut inflammation. a, Frequencies of RORγ$^+$Helios$^-$ in the colonic FOXP3$^+$CD4$^+$TCRβ$^+$ T_{reg} cell population on day 2 of DSS-induced colitis in mice fed a nutrient-rich diet, a minimal diet, or a minimal diet supplemented with mixtures of primary or secondary BAs in drinking water. The primary BAs were CA, CDCA and UDCA (2 mM of each). The secondary BAs were DCA, LCA, 3-oxo-CA, 3-oxo-LCA, 7-oxo-CA, 7-oxo-CDCA, 12-oxo-CA and 12-oxo-DCA (1 mM of each). **b**, Daily weight loss of mice described in **a** during the course of DSS-induced colitis. **c**, **d**, Clinical scores (**c**) and haematoxylin and eosin-stained histological sections (**d**) for representative colons on day 10 of colitis (see **b**). **e**, Daily weight loss of *Vdr*$^{flox/flox}$ and *Vdr*$^{flox/flox}$*Foxp3*$^{YFP\text{-}cre}$ mice during the course of DSS-induced colitis. **f**, Clinical scores for representative colons on day 10 of colitis (see **e**). Data are representative of two or three independent experiments. *n* represents biologically independent animals. Data are mean ± s.e.m. (**a**–**c**, **e** and **f**). $^*P < 0.05$, $^{**}P < 0.01$, $^{***}P < 0.001$, one-way ANOVA (**a** and **c**) or two-way ANOVA (**b** and **e**) followed by the Bonferroni post hoc test, or two-tailed Student's *t*-test (**f**).

BAs were sufficient to rescue colonic frequencies of RORγ$^+$ T_{reg} cells in minimal-diet NR1H4-deficient mice and their littermate controls (Fig. 3d). However, the failure of BA supplementation to restore colonic RORγ$^+$ T_{reg} cell counts in both minimal-diet VDR-deficient mice and minimal-diet mice deficient in both VDR and NR1H4 (Fig. 3d) implied a major role for the microbial BA–VDR axis in the regulation of colonic RORγ$^+$ T_{reg} cell populations.

As 1,25-dihydroxyvitamin D_3 can also activate VDR[19], we compared its levels in sera and colonic tissues from rich-diet and minimal-diet SPF mice and rich-diet GF mice. We found comparable levels among these three groups of mice (Extended Data Fig. 7a, b). We also found that, as previously reported[9], dietary vitamin A deficiency led to a decrease in the number of colonic RORγ$^+$ T_{reg} cells, while the absence of dietary vitamin D_3 did not have a similar effect (Extended Data Fig. 7c, d). These data indicated that the BA–VDR axis, not the vitamin D_3–VDR axis, is crucial in modulating RORγ$^+$ T_{reg} cells in the gut.

Next, we investigated which cell type responds to BA by affecting the upregulation of RORγ$^+$ T_{reg} cells. RNA sequencing (RNA-seq) performed on colonic-sorted cell fractions revealed high *Vdr* expression in epithelial and dendritic cells but also in FOXP3$^+$ T_{reg} cells—at a higher level than in T conventional (T_{conv}) cells (Fig. 3e). Indeed, *Vdr* expression is higher in colonic T_{reg} cells than in splenic T_{reg} cells, especially in RORγ$^+$ T_{reg} cells (Fig. 3f). This result is consistent with our earlier single-cell analysis highlighting VDR as a transcriptional regulator in colonic T_{reg} cells but not in other tissue T_{reg} cells[21]. To directly assess relevance, we crossed *Vdr*$^{flox/flox}$ conditional knockout mice with different Cre drivers to excise *Vdr* in distinct cell types. Colonic RORγ$^+$ T_{reg} cell counts were markedly reduced in *Vdr*$^{flox/flox}$*Foxp3*$^{YFP\text{-}cre}$ mice, while loss of VDR in dendritic or epithelial cells (*Cd11c*^{cre} and *Vil1*^{cre}; *Cd11c* is also known as *Itgax*) had no effect (Fig. 3g), demonstrating that VDR modulates colonic RORγ$^+$ T_{reg} cells in an intrinsic manner. RNA-seq profiling of colonic T_{reg} cells from VDR-deficient mice or control littermates showed a marked reduction in the transcriptional signature of colonic T_{reg} cells[8] in the absence of VDR (Fig. 3h); the RORγ$^+$ T_{reg} cell-specific signature was also downregulated, as expected (Extended Data Fig. 8). These data suggest that VDR is important in determining the RORγ-dependent program in colonic T_{reg} cells.

RORγ$^+$ T_{reg} cells have been reported to maintain colonic homeostasis and minimize colitis severity[8,11,22,23]. We investigated whether intestinal BAs modulate colonic inflammatory responses in a dextran sodium sulfate (DSS)-induced murine model of colitis. We saw no sign of inflammation in the colons of unchallenged mice fed a nutrient-rich diet, a minimal diet, or a minimal diet supplemented with primary or secondary BA mixtures in drinking water (Extended Data Fig. 9a–c). However, at the onset of colitis, challenged minimal-diet mice had a reduced proportion of colonic RORγ$^+$ T_{reg} cells (Fig. 4a)—an indication that they might be predisposed to severe colitis. Indeed, as DSS-induced colitis progressed, minimal-diet mice lost more weight and experienced more-severe colitis than rich-diet mice (Fig. 4b–d). Notably, both primary and secondary BA supplementation increased RORγ$^+$ T_{reg} cell counts in minimal-diet mice (Fig. 4a) and alleviated their colitis symptoms and signs (Fig. 4b–d). However, after colitis onset, BA supplementation barely alleviated colitis in minimal-diet mice (Extended Data Fig. 9d, e), suggesting that maintenance of an RORγ$^+$ T_{reg} cell pool by BAs during homeostasis is crucial to host resistance to DSS colitis. We next explored whether the BA–VDR axis is involved in regulating colitis in

mice. As in minimal-diet mice, deficiency of VDR in mice worsened the DSS-induced colitis phenotype (Extended Data Fig. 10a–c). The protective role of VDR signalling was also consistently observed in another mouse colitis model: naive $CD4^+$ T cell adaptive transfer into RAG1-deficient mice (Extended Data Fig. 10d–g). Importantly, severe DSS-induced colitis developed in *Vdr*$^{flox/flox}$*Foxp3*$^{YFP\text{-}cre}$ mice (Fig. 4e, f), implying that the BA–VDR axis has an intrinsic role in T_{reg} cell control of colonic inflammation.

As important molecular mediators, intestinal BAs are critical in maintaining a healthy colonic RORγ$^+$ T_{reg} cell pool through BARs. Gut bacteria differ in the types and quantities of BA derivatives they can generate. For instance, across different phyla, many gut bacterial species harbour genes encoding BSH that are involved in the primary BA deconjugation process. As their regulation and substrate specificity may vary, both primary and secondary BA metabolic profiles of these bacteria are likely to be affected[2,15]. In addition, the microbial diversity of secondary BA metabolism adds another layer of complexity to BA derivative production in individual species that may ultimately affect their capacity for RORγ$^+$ T_{reg} cell induction.

In view of the complexity of BA derivatives, our study suggests that dominant intestinal primary BA species—for example, cholic/chenodeoxycholic/ursodeoxycholic acids—along with certain potent secondary BA species—for example, lithocholic/3-oxo-lithocholic acids—modulate RORγ$^+$ T_{reg} cells through the BAR VDR. Dysregulation of intestinal BAs has been proposed as a mediator of the pathogenesis of human inflammatory bowel diseases and colorectal cancers[1,24]. The essential role of VDR in modulating peripheral RORγ$^+$ T_{reg} cells and colitis susceptibility raises the interesting possibility that human *VDR* genetic variants associated with inflammatory bowel diseases[25] might affect disease susceptibility through improper control of the intestinal T_{reg} cell pool. Mechanistically, it is intriguing to speculate that the nuclear receptor VDR—a colonic T_{reg} cell-preferring transcription factor[21]—may modulate colonic T_{reg} cell homeostasis by coordinating BA signals with transcription factor activity. An understanding of the molecular mechanisms underlying the regulation of colonic T_{reg} cells by this biliary network between hosts and their associated microorganisms will be valuable in improving therapy for human gastrointestinal inflammatory disorders.

Online content

Any methods, additional references, Nature Research reporting summaries, source data, extended data, supplementary information, acknowledgements, peer review information; details of author contributions and competing interests; and statements of data and code availability are available at https://doi.org/10.1038/s41586-019-1865-0.

1. Postler, T. S. & Ghosh, S. Understanding the holobiont: how microbial metabolites affect human health and shape the immune system. *Cell Metab.* **26**, 110–130 (2017).
2. Ridlon, J. M., Kang, D. J. & Hylemon, P. B. Bile salt biotransformations by human intestinal bacteria. *J. Lipid Res.* **47**, 241–259 (2006).
3. Wahlström, A., Sayin, S. I., Marschall, H. U. & Bäckhed, F. Intestinal crosstalk between bile acids and microbiota and its impact on host metabolism. *Cell Metab.* **24**, 41–50 (2016).
4. Fiorucci, S. & Distrutti, E. Bile acid-activated receptors, intestinal microbiota, and the treatment of metabolic disorders. *Trends Mol. Med.* **21**, 702–714 (2015).
5. Brestoff, J. R. & Artis, D. Commensal bacteria at the interface of host metabolism and the immune system. *Nat. Immunol.* **14**, 676–684 (2013).
6. Tanoue, T., Atarashi, K. & Honda, K. Development and maintenance of intestinal regulatory T cells. *Nat. Rev. Immunol.* **16**, 295–309 (2016).
7. Panduro, M., Benoist, C. & Mathis, D. Tissue Tregs. *Annu. Rev. Immunol.* **34**, 609–633 (2016).
8. Sefik, E. et al. Mucosal immunology. Individual intestinal symbionts induce a distinct population of RORγ$^+$ regulatory T cells. *Science* **349**, 993–997 (2015).
9. Ohnmacht, C. et al. Mucosal immunology. The microbiota regulates type 2 immunity through RORγt$^+$ T cells. *Science* **349**, 989–993 (2015).
10. Geva-Zatorsky, N. et al. Mining the human gut microbiota for immunomodulatory organisms. *Cell* **168**, 928–943 (2017).
11. Xu, M. et al. c-MAF-dependent regulatory T cells mediate immunological tolerance to a gut pathobiont. *Nature* **554**, 373–377 (2018).
12. Yissachar, N. et al. An intestinal organ culture system uncovers a role for the nervous system in microbe–immune crosstalk. *Cell* **168**, 1135–1148 (2017).
13. Kim, K. S. et al. Dietary antigens limit mucosal immunity by inducing regulatory T cells in the small intestine. *Science* **351**, 858–863 (2016).
14. Sayin, S. I. et al. Gut microbiota regulates bile acid metabolism by reducing the levels of tauro-beta-muricholic acid, a naturally occurring FXR antagonist. *Cell Metab.* **17**, 225–235 (2013).
15. Yao, L. et al. A selective gut bacterial bile salt hydrolase alters host metabolism. *eLife* **7**, e37182 (2018).
16. Devlin, A. S. & Fischbach, M. A. A biosynthetic pathway for a prominent class of microbiota-derived bile acids. *Nat. Chem. Biol.* **11**, 685–690 (2015).
17. Wexler, A. G. & Goodman, A. L. An insider's perspective: *Bacteroides* as a window into the microbiome. *Nat. Microbiol.* **2**, 17026 (2017).
18. Stevens, A. M., Shoemaker, N. B. & Salyers, A. A. The region of a *Bacteroides* conjugal chromosomal tetracycline resistance element which is responsible for production of plasmidlike forms from unlinked chromosomal DNA might also be involved in transfer of the element. *J. Bacteriol.* **172**, 4271–4279 (1990).
19. Makishima, M. et al. Vitamin D receptor as an intestinal bile acid sensor. *Science* **296**, 1313–1316 (2002).
20. Makishima, M. et al. Identification of a nuclear receptor for bile acids. *Science* **284**, 1362–1365 (1999).
21. DiSpirito, J. R. et al. Molecular diversification of regulatory T cells in nonlymphoid tissues. *Sci. Immunol.* **3**, eaat5861 (2018).
22. Yang, B. H. et al. Foxp3$^+$ T cells expressing RORγt represent a stable regulatory T-cell effector lineage with enhanced suppressive capacity during intestinal inflammation. *Mucosal Immunol.* **9**, 444–457 (2016).
23. Britton, G. J. et al. Microbiotas from humans with inflammatory bowel disease alter the balance of gut Th17 and RORγt$^+$ regulatory T cells and exacerbate colitis in mice. *Immunity* **50**, 212–224 (2019).
24. Staley, C., Weingarden, A. R., Khoruts, A. & Sadowsky, M. J. Interaction of gut microbiota with bile acid metabolism and its influence on disease states. *Appl. Microbiol. Biotechnol.* **101**, 47–64 (2017).
25. Xue, L. N. et al. Associations between vitamin D receptor polymorphisms and susceptibility to ulcerative colitis and Crohn's disease: a meta-analysis. *Inflamm. Bowel Dis.* **19**, 54–60 (2013).

Methods

Mice and dietary treatments

C57BL/6J wild-type mice were obtained from Jackson, as were *Vdr*$^{-/-}$, *Nr1h3*$^{-/-}$, *Nr1h4*$^{-/-}$, *Chrm2*$^{-/-}$, *Chrm3*$^{-/-}$, *Rag1*$^{-/-}$, *Foxp3*$^{YFP\text{-}cre}$, *Cd11c*^{cre}, *Vil1*^{cre} and *Foxp3*^{mRFP} mice. *Nr1i2*$^{-/-}$*Nr1i3*$^{-/-}$ mice were obtained from Taconic. *Gpbar1*$^{-/-}$ mice were purchased from KOMP Repository. *S1pr2*$^{-/-}$ mice were provided by T. Hla (Boston Children's Hospital). *Vdr*$^{flox/flox}$ mice[26] were provided by D. Gardner (University of California, San Francisco) and then crossed with *Foxp3*$^{YFP\text{-}cre}$, *Cd11c*^{cre} or *Vil1*^{cre} mice to generate the corresponding cell-type-specific knockout mice. *Vdr*$^{-/-}$*Nr1h4*$^{-/-}$ mice were obtained by crossing *Vdr*$^{+/-}$ with *Nr1h4*$^{+/-}$ mice. *Vdr*$^{+/+}$*Foxp3*^{mRFP} or *Vdr*$^{-/-}$*Foxp3*^{mRFP} reporter mice were generated by crossing *Vdr*$^{+/-}$ with *Foxp3*^{mRFP} reporter mice. Sterilized vitamin A-deficient, vitamin D_3-deficient and control diets on a nutrient-rich diet background were purchased from TestDiet. For dietary treatment experiments with BA supplementation, 3-week-old C57BL/6J wild-type mice were fed either a sterilized nutrient-rich diet (LabDiet 5K67) or a minimal diet (TestDiet AIN-76A) for 4 weeks. Some groups of the mice fed a minimal diet were also treated with various BAs (sodium salt form) in drinking water for 4 weeks as described below. The primary BAs tested were cholic acid, chenodeoxycholic acid and ursodeoxycholic acid (2 mM or 6 mM of a single BA); a mixture of cholic acid and chenodeoxycholic acid (3 mM of each, 6 mM in total); a mixture of cholic acid and ursodeoxycholic acid (3 mM of each, 6 mM in total); a mixture of chenodeoxycholic acid and ursodeoxycholic acid (3 mM of each, 6 mM in total); and a mixture of cholic acid, chenodeoxycholic acid and ursodeoxycholic acid (2 mM of each, 6 mM in total). The secondary BAs tested were deoxycholic acid, lithocholic acid, 3-oxo-cholic acid, 3-oxo-lithocholic acid, 7-oxo-cholic acid, 7-oxo-chenodeoxycholic acid, 12-oxo-cholic acid and 12-oxo-deoxycholic acid (2 mM of a single BA); a mixture of deoxycholic acid and lithocholic acid (2 mM of each, 4 mM in total); a mixture of lithocholic acid and 3-oxo-lithocholic acid (2 mM of each, 4 mM in total); a mixture of deoxycholic acid, 3-oxo-cholic acid, 7-oxo-cholic acid and 12-oxo-cholic acid (2 mM of each, 8 mM in total); a mixture containing the oxo-BAs (1 mM of each, 6 mM in total); and a mixture containing the oxo-BAs, deoxycholic acid and lithocholic acid (1 mM of each, 8 mM in total). Three-week-old mice fed a minimal diet were also treated with SCFAs (sodium salt form) in drinking water. The SCFAs tested were acetate and propionate (36 mM or 150 mM of either SCFA); butyrate (36 mM or 100 mM); and a combination of acetate, propionate and butyrate (36 mM of each, 108 mM in total). Fresh drinking water was supplied each week. Pregnant C57BL/6J wild-type mice were also fed a sterilized nutrient-rich diet or a minimal diet during gestation and nursing, and their offspring were exposed to the same diet until weaning at approximately 3 weeks of age. The offspring were then fed the same diet as their dams or switched to the opposite diet for another 4 weeks before phenotype analysis. Occasional growth restriction in mice fed a minimal diet necessitated their exclusion from all experiments. All mice were housed under the same conditions in SPF facilities at Harvard Medical School (HMS), and littermates from each mouse line were bred as strict controls. GF C57BL/6 mice were obtained from the National Gnotobiotic Rodent Resource Center at the University of North Carolina at Chapel Hill and were maintained in GF isolators at HMS. Animal protocol IS00000187-3 and COMS protocol 07-267 were approved by the HMS Institutional Animal Care and Use Committee and the Committee on Microbiological Safety, respectively. All animal studies were performed in compliance with the guidelines of ARRIVE.

Anaerobic bacterial culture

B. thetaiotaomicron VPI-5482 and *B. fragilis* 638R were grown either on basal medium (protease peptone, 20 g l^{-1}; yeast extract, 5 g l^{-1}; and NaCl, 5 g l^{-1}) supplemented with 0.5% glucose, 0.5% K_2HPO_4, 0.05% L-cysteine, 5 mg l^{-1} haemin and 2.5 mg l^{-1} vitamin K_1, or on BBL Brucella agar with 5% sheep blood, haemin and vitamin K_1. The bacteria were then cultured under strictly anaerobic conditions (80% N_2, 10% H_2 and 10% CO_2) at 37 °C in an anaerobic chamber.

Genetical manipulation of bacteria

Deletion mutants of *B. thetaiotaomicron* VPI-5482 were created by removal of the genes encoding BSHs (BT_1259 and BT_2086), the gene encoding 7α-HSDH (BT_1911) or all three genes. Deletion mutants of *B. fragilis* 638R were created by removal of the gene encoding BSH (BF638R_3610), the gene encoding 7α-HSDH (BF638R_3349) or both genes. DNA segments (1 kb) upstream and downstream of the region to be deleted were PCR amplified with the following primers: BT_1259 up forward: 5′-TTTGTCGACTTATATTTTCTTCCAAAACT-3′; BT_1259 up reverse: 5′-CAAGCTGCTATCAATAATTTCGATTTTTAGTTATA-3′; BT_1259 down forward: 5′-CTAAAAATCGAAATTATTGATAGCAGCTTGCTGCA-3′; BT_1259 down reverse: 5′-TTTGGATCCGGGAGGATTCCACATAATAT-3′; BT_2086 up forward: 5′-TTTGTCGACCATCCAAACCCAGTGTGAAC-3′; BT_2086 up reverse: 5′-ATAACTAACTATCGAATTACTTCCAAATTAAATAG-3′; BT_2086 down forward: 5′-TAATTTGGAAGTAATTCGATAGTTAGTTATGTGGT-3′; BT_2086 down reverse: 5′-TTTGGATCCAAGAGCATAAAGAGCTGTTG-3′; BT_1911 up forward: 5′-TTTGTCGACTAGGAAAAGAAAAAGTGATC-3′; BT_1911 up reverse: 5′-CTGTCCGGGGTATATATATGTTGAGAATTTGATGA-3′; BT_1911 down forward: 5′-AAATTCTCAACATATATATACCCCGGACAGTACAT-3′; BT_1911 down reverse: 5′-TTTGGATCCAATTTGATATAAGCGTACGA-3′; BF638R_3610 up forward: 5′-TTTGTCGACTATAGCTGGATGGCTGTTGC-3′; BF638R_3610 up reverse: 5′-CCTCGGTAGACATTTACTCTTTATATTAAAATGGT-3′; BF638R_3610 down forward: 5′-TTTAATATAAAGAGTAAATGTCTACCGAGGCAGAT-3′; BF638R_3610 down reverse: 5′-TTTGGATCCAGAAGAAGAGATTGGTTCAC-3′; BF638R_3349 up forward: 5′-TTTGTCGACATCCCCGCCTGAGCAAGAAG-3′; BF638R_3349 up reverse: 5′-TTGATAAGATTCTTTAATAGGATGGTTTTGAGGAT-3′; BF638R_3349 down forward: 5′-CAAAACCATCCTATTAAAGAATCTTATCAAGTTAC-3′; BF638R_3349 down reverse: 5′-TTTGGATCCCCTGAGGGGTGGGAGAAACT-3′. PCR products from upstream and downstream regions were further fused together by fusion PCR to generate 2-kb PCR products, which were digested with BamHI and SalI. The digested products were cloned into the appropriate site of the *Bacteroides* suicide vector pNJR6. The resulting plasmids were conjugally transferred into *Bacteroides* strains by the helper plasmid R751, and *Bacteroides* strains integrated with the plasmids were selected by erythromycin resistance. The integrated *Bacteroides* strains were passaged for ten generations without erythromycin selection, and cross-out mutants were determined by PCR with primers targeting the two flanking regions of the indicated genes. PCR of an intact gene plus its flanking regions generated a product of approximately 1,150–1,500 bp, while successful deletion of the gene of interest resulted in a PCR amplicon of only 350–450 bp of its two flanking regions. The DKO mutant of *B. fragilis* and the TKO mutant of *B. thetaiotaomicron* were created by subsequent deletion of the indicated genes.

Generation of monocolonized mice

GF C57BL/6J mice were orally inoculated by gavage with a broth-grown single bacterial strain at 4 weeks of age. Each group of mice was then maintained in a gnotobiotic isolator under sterile conditions for 2 weeks. Faecal material was collected and plated 2 weeks after bacterial inoculation to determine colonization levels (colony-forming unit per gram of faeces) and to ensure colonization by a single bacterial strain.

BA extraction and quantification

Faecal contents from the distal colons of mice were collected and weighed before BA extraction[27]. In brief, one weighed faecal pellet was resuspended with 500 µl sterile ddH_2O in a 1.5-ml screw-cap conical tube and sonicated for 10 min. The homogenates were centrifuged at 300*g* for 5 min, and the supernatants were transferred to a new tube. The remaining material was resuspended in 250 µl LC–MS-grade methanol

containing internal standards and subjected to sonication for another 10 min. The homogenates were also centrifuged at 300*g* for 5 min and the supernatants were collected and combined, after which another 500-µl volume of sterile ddH_2O was added to make a final 1.25-ml solution. The solution was acidified with acetic acid (Sigma) and then loaded onto a methanol-activated C18 column. The column was subsequently washed with 1 ml of 85:15 (vol/vol) H_2O/methanol solution, and the BAs were eluted with 2 ml of 25:75 (vol/vol) H_2O/methanol solution. The eluted solutions were dried under nitrogen and resuspended in 200 µl of 50:50 (vol/vol) H_2O/acetonitrile solution. The samples were kept at −20 °C until analysed. Nineteen synthetic standards (taurocholic acid, taurochenodeoxycholic acid, tauroursodeoxycholic acid, cholic acid, chenodeoxycholic acid, ursodeoxycholic acid, lithocholic acid and deoxycholic acid from Sigma; tauro-α-muricholic acid, tauro-β-muricholic acid, β-muricholic acid and ω-muricholic acid from Santa Cruz; and α-muricholic acid, 3-oxo-cholic acid, 3-oxo-lithocholic acid, 7-oxo-cholic acid, 7-oxo-chenodeoxycholic acid, 12-oxo-cholic acid and 12-oxo-deoxycholic acid from Steraloids) were run, and a calibration curve was generated for quantification. All standards were resuspended in LC–MS-grade acetonitrile and prepared in-phase for analysis. All samples and standards were analysed by ultra-performance liquid chromatography coupled to electrospray ionization tandem mass spectrometry (UPLC–ESI-MS/MS; Thermo Scientific Orbitrap Q Exactive with Thermo Vanquish UPLC) with a Phenomenex Kinetex C8 (100 mm × 3 mm × 1.7 µm) column; a 20–95% gradient of H_2O-acetonitrile was used as eluent, with 0.1% formic acid as an additive. Mass spectral data were acquired by a cycle of MS1 scan (range 300–650), followed by data-dependent MS/MS scanning (ddMS2) of the top 5 ions in the pre-generated inclusion list. D_4-glycocholic acid and D_4-deoxycholic acid served as internal standards for conjugated and unconjugated BAs, respectively.

SCFA extraction and quantification

Faecal contents from the distal colons of mice were collected and weighed before SCFA extraction. Faecal contents were resuspended in 75% acetonitrile containing three deuterated internal standards (D_3-acetate, D_5-propionate and D_7-butyrate). Samples were sonicated for 10 min, vortexed and centrifuged at 8,000*g* for 5 min. Supernatant was collected and treated with activated charcoal to remove non-polar lipids by re-centrifuging. Supernatant was then collected, dried under nitrogen and resuspended in 95% acetonitrile solution. The samples were kept at −20 °C until analysed. All standards were resuspended in UPLC-grade methanol. For hydrophilic interaction liquid chromatography (HILIC)–ESI-MS/MS analysis, a Waters BEH amide HILIC column (2.1 mm × 100 mm × 2.5 µm) was used with a linear gradient of acetonitrile:H_2O = 95:5 to 60:40 (vol/vol) with 2 mM ammonium formate at pH 9.0. Deprotonated anion ($[M-H]^-$) of each SCFA (acetate, propionate and butyrate) was quantitated in negative-ion mode.

MS data acquisition and processing

Each individual species has been matched with its (1) accurate MS1 anion ($[M-H]^-$ or $[M+HCOO^-]$), (2) isotope ratio, and (3) LC retention time of authentic standard, for suitable identification and quantification of level 1 metabolite[28]. Thermo Xcalibur Suite version 3.0 was used for peak identification and area integration as well as generation of a calibration curve for all synthetic standards. Raw data (integrated ion counts) were converted to absolute amounts by the calibration curve of individual species. Recovery of internal standards of individual samples was also calculated in same procedure. The calculated value was normalized by sample weight and the proportion of the injected sample for analysis to generate the desired final concentration (µg per g or µmol per g sample).

Isolation of mouse lymphocytes and flow cytometry

For isolation of lamina propria lymphocytes, colonic and small-intestinal tissues were dissected and fatty portions discarded. Peyer's patches were also removed from the small intestines for isolation of lymphocytes. The excised intestinal tissues were washed in cold PBS buffer, and epithelia were removed by 500-r.p.m. stirring at 37 °C in RPMI medium (Gibco) containing 1 mM EDTA (Ambion), 1 mM dithiothreitol (Sigma) and 2% (vol/vol) FBS (GemBio). After 15 min of incubation, the epithelium-containing supernatants were discarded, and the remaining intestinal tissues were washed in RPMI medium with 5% (vol/vol) FBS, further minced into small pieces, and digested by 500-r.p.m. stirring at 37 °C in RPMI medium containing collagenase type II (1.5 mg ml^{-1}, Invitrogen), Dispase II (0.5 mg ml^{-1}, Invitrogen) and 1.2% (vol/vol) FBS for 40 min. The digested tissues were filtered, and the solutions were centrifuged at 500*g* for 10 min to collect lamina propria cells. The pellets were resuspended, and the lamina propria lymphocytes were isolated by GE Healthcare Percoll (40%/80%) gradient centrifugation. For isolation of Peyer's patch lymphocytes, the excised Peyer's patches were digested in the same medium by 500-r.p.m. stirring at 37 °C for 10 min, the digested Peyer's patches were filtered, the solutions were centrifuged at 500*g* for 10 min and lymphocytes were collected. Lymph nodes, spleens and thymuses were mechanically disrupted. Single-cell suspensions were subjected to flow cytometric analysis by staining with antibodies against CD45 (30-F11, BioLegend), CD4 (GK1.5, BioLegend), TCRβ (H57-597, BioLegend), Helios (22F6, BioLegend), RORγ (AFKJS-9, eBioscience) and FOXP3 (FJK-16s, eBioscience). For intracellular staining of transcription factors, cells were blocked with an antibody against CD16/32 (2.4G2, BD Pharmingen) and stained for surface and viability markers. Fixation of cells in eBioscience Fix/Perm buffer for 50 min at room temperature was followed by permeabilization in eBioscience permeabilization buffer for 50 min in the presence of antibodies at room temperature. Cells were acquired with a Miltenyi MACSQuant Analyzer, and analysis was performed with FlowJo software.

Murine colitis models and histology

Three-week-old C57BL/6J wild-type mice were fed a sterilized nutrient-rich diet or a minimal diet for 4 weeks. Some groups of the mice fed a minimal diet were also pre-treated with a bile-salt mixture in drinking water for 4 weeks. The mice were next treated with 2.5% DSS (MP Biomedicals) in drinking water for 5 days and then switched back to regular water or bile salt-containing water for another 5 days[29]. $Vdr^{+/+}$, $Vdr^{-/-}$, $Vdr^{flox/flox}$ and $Vdr^{flox/flox}Foxp3^{YFP\text{-}cre}$ mice were treated with 2.5% DSS by the same protocol. The mice were weighed throughout the course of experimental colitis and were killed at specific time points, after which colonic tissue was obtained for histopathological and FACS analyses. For the T cell-adoptive transfer model of colitis[29], the indicated splenic naive T cells ($TCR\beta^+CD4^+CD25^-CD45RB^{hi}$) were sorted from 8-week-old $Vdr^{+/+}$ and $Vdr^{-/-}$ mice by flow cytometry (Astrios, BD Biosciences). Cells (5×10^5 in 200 µl sterile PBS) were then intraperitoneally injected into $Rag1^{-/-}$ recipient mice. The mice were weighed throughout the T cell colitis model to assess their weight loss. Colonic tissues from both colitis models were dissected and immediately fixed with Bouin's fixative solution (RICCA) for histological analyses. Paraffin-embedded sections of colonic tissue were stained with haematoxylin and eosin, and clinical scores were determined by light microscopy[30].

RNA isolation and quantitative PCR

Total RNA was extracted from mouse colonic tissues with TRIzol reagent (Invitrogen) according to the manufacturer's instructions. RNA samples were reverse-transcribed into cDNA with a TaKaRa PrimeScript RT Reagent Kit. The cDNA samples were amplified by quantitative PCR with a KAPA SYBR FAST qPCR kit on an Eppendorf Realplex^2 Mastercycler. The primers for quantitative PCR were as follow: *Vdr* forward: 5′-CACCTGGCTGATCTTGTCAGT-3′; *Vdr* reverse: 5′-CTGGTCATCAGAGG TGAGGTC-3′; *Nr1h3* forward: 5′-TGTGCGCTCAGCTCTTGT-3′; *Nr1h3* reverse: 5′-TGGAGCCCTGGACATTACC-3′; *Nr1h4* forward: 5′-GAAAATCC AATTCAGATTAGTCTTCAC-3′; *Nr1h4* reverse: 5′-CCGCGTGTTCTGTT AGCAT-3′; *Nr1i2* forward: 5′-TCTCAGGTGTTAGGTGGGAGA-3′; *Nr1i2*

reverse: 5′-GCACGGGGGTACAACTGTTA-3′; *Nr1i3* forward: 5′-AAATGTTGGCATGAGGAAAGA-3′; *Nr1i3* reverse: 5′-CTGATTCAGTTGCAAAGATGCT-3′; *Gpbar1* forward: 5′-ATTCCCATGGGGGTTCTG-3′; *Gpbar1* reverse: 5′-GAGCAGGTTGGCGATGAC-3′; *Chrm2* forward: 5′-AAAGGCTCCTCGCTCCAG-3′; *Chrm2* reverse: 5′-AGTCAAGTGGCCAAAGAAACA-3′; *Chrm3* forward: 5′-ACTGGACAGTCCGGGAGATT-3′; *Chrm3* reverse: 5′-TGCCATTGCTGGTCATATCT-3′; *S1pr2* forward: 5′-CCCAACTCCGGGACATAGA-3′; *S1pr2* reverse: 5′-ACAGCCAGTGGTTGGTTTTG-3′; *Rpl13a* forward: 5′-GGGCAGGTTCTGGTATTGGAT-3′; *Rpl13a* reverse: 5′-GGCTCGGAAATGGTAGGGG-3′. Expression of the indicated genes was normalized to the expression of housekeeping gene *Rpl13a*.

16S rRNA profiling of the gut microbiota

Faecal DNA was extracted from faecal pellets of the indicated mice with a QIAGEN QIAamp Fast DNA Stool Mini Kit (ref. no. 51604) according to the manufacturer's instructions. The DNA samples were stored at −80 °C before processing. Purified DNA samples were quantified with a Qubit dsDNA HS Assay Kit (Invitrogen, Q32854) and normalized to 6 ng μl^{-1}, with subsequent amplification with barcoded primer pairs: 515f PCR forward primer: 5′-AATGATACGGCGACCACCGAGAT CTACACGCT TATGGTAATT GT GTGCCAGCMGCCGCGGTAA-3′; 806r PCR reverse primer: 5′-CAAGCAGAAGACGGCATACGAGAT XXXXXXXXXXXXAGTCAGTCAG CC GGACTACHVGGGTWTCTAAT-3′ (with XXXXXXXXXXXX representing the barcodes). PCR products were quantified with the above Qubit kit and then combined into a pool library with equal mass to each sample. The pooled library was purified by AMpure beads (Beckman Coulter, A63880) and then subjected to agarose gel electrophoresis. A DNA band of approximately 390 bp was dissected and purified with a QIAquick Gel Extraction Kit (Qiagen, 28704). The concentration of the pooled library was measured and normalized to 10 nM. The purified pooled DNA library was qualified by an Agilent High Sensitivity DNA Chip on a bioanalyzer. The quantitated library was then subjected to multiplex sequencing (Illumina MiSeq, 251 nt × 2 pair-end reads with 12-nt index reads). Raw sequencing data were analysed by QIIME2. In brief, the data were imported into QIIME2 and demultiplexed, a DADA2 pipeline was used for sequencing quality control, and a feature table was constructed with the following options: qiime dada2 denoise-paired −i-demultiplexed-seqs demux.qza −o-table table −o-representative-sequences rep-seqs −p-trim-left-f 0 −p-trim-left-r 0 −p-trunc-len-f 150 −p-trunc-len-r 150. The feature table of the gut microbiota was used for alpha and beta diversity analysis as well as for taxonomic analysis and differential abundance testing.

Faecal bacterial DNA extraction and quantitative PCR analysis

Faecal DNA was extracted from the faecal pellets of indicated mice with a QIAGEN QIAamp Fast DNA Stool Mini Kit (51604) according to the manufacturer's instructions. Quantitative PCR analysis was performed with an Eppendorf Realplex^2 Mastercycler and a KAPA SYBR FAST qPCR Kit. The 16S rRNA gene primers for real-time quantitative PCR were as follows[31]: total bacteria forward: 5′-GGTGAATACGTTCCCGG-3′; total bacteria reverse: 5′-TACGGCTACCTTGTTACGACTT-3′; *Clostridium* cluster IV forward: 5′-CCTTCCGTGCCGSAGTTA-3′; *Clostridium* cluster IV reverse: 5′-GAATTAAACCACATACTCCACTGCTT-3′; *Clostridium* cluster XIVα forward: 5′-AAATGACGGTACCTGACTAA-3′; *Clostridium* cluster XIVα reverse: 5′-CTTTGAGTTTCATTCTTGCGAA-3′. The relative quantity of the indicated *Clostridium* clusters was normalized to the total bacteria.

RNA-seq and microarray analysis of splenic and colonic cells

Mouse colonic lymphocytes form *Vdr*$^{+/+}$*Foxp3*^{mRFP} or *Vdr*$^{-/-}$*Foxp3*^{mRFP} reporter mice were isolated as described above. Single-cell suspensions were blocked with an antibody against CD16/32 (2.4G2) and stained with antibodies against BioLegend CD45 (30-F11), CD4 (GK1.5), TCRβ (H57-597), CD8α (53-6.7), CD19 (1D3/CD19), CD11c (N418), F4/80 (BM8) and TER-119 (TER-119) and with viability dye. Live FOXP3$^+$ T_{reg} cells (CD45$^+$CD19$^-$CD11c$^-$F4/80$^-$TER-119$^-$TCRβ$^+$CD8α$^-$CD4$^+$mRFP$^+$) were double-sorted by flow cytometry (Astrios, BD Biosciences) to achieve 99% purity and directly lysed with TCL buffer (Qiagen, 1031576) containing 1% 2-mercaptoethanol (Sigma-Aldrich, M6250). Colonic live T_{conv} cells (CD45$^+$CD19$^-$CD11c$^-$F4/80$^-$TER-119$^-$TCRβ$^+$CD8α$^-$CD4$^+$mRFP$^-$) and CD11c$^+$ dendritic cells (CD45$^+$CD19$^-$TCRβ$^-$TER-119$^-$F4/80$^-$CD11c$^+$) were double-sorted at the same time. Colonic epithelial cells (CD45$^-$EpCAM$^+$) were also isolated as previously described[32]. Samples lysed in TCL buffer (Qiagen, 1031576) were kept on ice for 5 min, frozen by dye ice and stored at −80 °C before processing. Smart-Seq2 libraries for low-input RNA-seq were prepared by the Broad Technology Labs and were subsequently sequenced through the Broad Genomics Platform. In brief, total RNA was extracted and purified by Agencourt RNAClean XP beads (Beckman Coulter, A66514). mRNA was polyadenylated and selected by an anchored oligo (dT) primer and converted to cDNA by reverse transcription. First-strand cDNA was amplified by PCR followed by transposon-based fragmentation with the Nextera XT DNA Library Preparation Kit (Illumina, FC-131-1096). Samples were then amplified with barcoded primers (Illumina P5 and P7 barcodes) by PCR. Pooled samples were subjected to sequencing on an Illumina NextSeq500 (2 × 25-bp reads). Transcripts were quantified by the Broad Technology Labs computational pipeline (Cuffquant version 2.2.1[33]). Normalized reads were further filtered and analysed by Multiplot Studio in the GenePattern software package. The colonic T_{reg} cell signatures (fold change > 2 and $P < 0.05$) and RORγ$^+$ T_{reg} cell signatures (fold change > 1.5 and $P < 0.05$)[8] were used in the present study. Loss of VDR functional transcripts in all VDR-deficient cells was confirmed by analysis of a deletion of *Vdr* exon 3 transcripts in the cells[34].

Microarray analysis of splenic and colonic T_{reg} cells was described in our previous report (GEO accession: GSE68009)[8], and the expression of VDR within these populations is shown in the present study.

ELISA of mouse 1,25-dihydroxyvitamin D_3

SPF mice were fed either a nutrient-rich or a minimal diet, and GF mice were fed the nutrient-rich diet as described above. Whole blood was collected in a serum separation tube and allowed to clot for 2 h at room temperature. The serum was then collected by centrifugation at 10,000 r.p.m. for 15 min. Colonic tissues were dissected, weighed and then homogenized in 500 μl PBS on ice. The cells were lysed by freeze (liquid nitrogen)–thaw (room temperature) for three cycles, and the supernatants were collected by centrifugation at 13,000 r.p.m. for 15 min. Serum and colonic levels of 1,25-dihydroxyvitamin D_3 in the indicated mice were determined with a mouse 1,25-dihydroxyvitamin D_3 ELISA kit (LifeSpan BioSciences, LS-F28132) according to the manufacturer's instructions.

Immunoblot analysis

Mouse colonic tissues were directly lysed with Triton buffer (0.5% Triton X-100 and 20 mM HEPES, pH 7.6) on ice, and the lysates were separated by NuPAGE 4–12% Bis-Tris gel (Invitrogen). Separated proteins were transferred onto iBlot 2 NC Mini Stacks (Invitrogen) with an iBlot 2 Dry Blotting System (Invitrogen). The filters were then blocked with TBS with 5% non-fat dry milk (Rockland) plus 0.1% Tween 20 for 1 h at room temperature. After blocking, the filters were incubated overnight at 4 °C with primary antibodies (1:1,000 dilution) against VDR (sc-13133, Santa Cruz), NR1H4 (sc-25309, Santa Cruz), GPBAR1 (PA5-23182, Invitrogen) or actin (sc-8432, Santa Cruz), and were subsequently washed three times with TBS (Bio-Rad) containing 0.1% Tween 20 (Bio-Rad). The filters were then incubated with IRDye 680LT secondary antibodies (1:5,000 dilution) (LI-COR Biosciences) for 1 h at room temperature in the dark. After three washes with TBS containing 0.1% Tween 20, the indicated signals were detected with an Odyssey CLx Fluorescence Imaging System (LI-COR).

Statistical analysis

Results were shown as mean ± s.e.m. Differences between groups were evaluated by analysis of variance followed by a Bonferroni post hoc test or by two-tailed Student's *t*-test with 95% confidence intervals. To determine the enrichment of certain gene signatures in RNA-seq datasets, we used a χ^2 test. $P < 0.05$ was considered statistically significant.

Reporting summary

Further information on research design is available in the Nature Research Reporting Summary linked to this paper.

Data availability

The microarray, RNA-seq and 16S rRNA profiling data are available in the NCBI database under accession numbers GSE68009, GSE137405 and PRJNA573477, respectively. The MS data are available in the MetaboLights database with the identifier MTBLS1276.

26. Chen, S. et al. Cardiomyocyte-specific deletion of the vitamin D receptor gene results in cardiac hypertrophy. *Circulation* **124**, 1838–1847 (2011).
27. Persson, E. et al. Simultaneous assessment of lipid classes and bile acids in human intestinal fluid by solid-phase extraction and HPLC methods. *J. Lipid Res.* **48**, 242–251 (2007).
28. Sumner, L. W. et al. Proposed minimum reporting standards for chemical analysis Chemical Analysis Working Group (CAWG) Metabolomics Standards Initiative (MSI). *Metabolomics* **3**, 211–221 (2007).
29. Song, X. et al. Growth factor FGF2 cooperates with interleukin-17 to repair intestinal epithelial damage. *Immunity* **43**, 488–501 (2015).
30. Wirtz, S., Neufert, C., Weigmann, B. & Neurath, M. F. Chemically induced mouse models of intestinal inflammation. *Nat. Protocols* **2**, 541–546 (2007).
31. Atarashi, K. et al. Induction of colonic regulatory T cells by indigenous *Clostridium* species. *Science* **331**, 337–341 (2011).
32. Haber, A. L. et al. A single-cell survey of the small intestinal epithelium. *Nature* **551**, 333–339 (2017).
33. Trapnell, C. et al. Differential gene and transcript expression analysis of RNA-seq experiments with TopHat and Cufflinks. *Nat. Protocols* **7**, 562–578 (2012).
34. Li, Y. C. et al. Targeted ablation of the vitamin D receptor: an animal model of vitamin D-dependent rickets type II with alopecia. *Proc. Natl Acad. Sci. USA* **94**, 9831–9835 (1997).

Acknowledgements We thank D. Gardner, Y. Li and T. Hla for providing mouse strains, and C. Fu for help with microscope. We also thank T. Sherpa and J. Ramos for help with GF mice and J. McCoy for manuscript editing. This work was supported in part by a Sponsored Research Agreement from UCB Pharma and Evelo Biosciences. S.F.O. was supported by NIH K01 DK102771.

Author contributions D.L.K. and X. Song designed the experiments and wrote the manuscript. X. Song, X. Sun, S.F.O., M.W., Y.Z., W.Z. and N.G.-Z. conducted or helped with the experiments. X. Song, X. Sun and Y.Z. analysed the data. R.J., D.M. and C.B. were involved in data discussions and edited the manuscript. D.L.K. supervised the study.

Competing interests The authors declare no competing interests.

Additional information
Supplementary information is available for this paper at https://doi.org/10.1038/s41586-019-1865-0.
Correspondence and requests for materials should be addressed to D.L.K.
Peer review information *Nature* thanks Pieter Dorrestein, Hiroshi Ohno and the, other, anonymous reviewer(s) for their contribution to the peer review of this work.
Reprints and permissions information is available at http://www.nature.com/reprints.

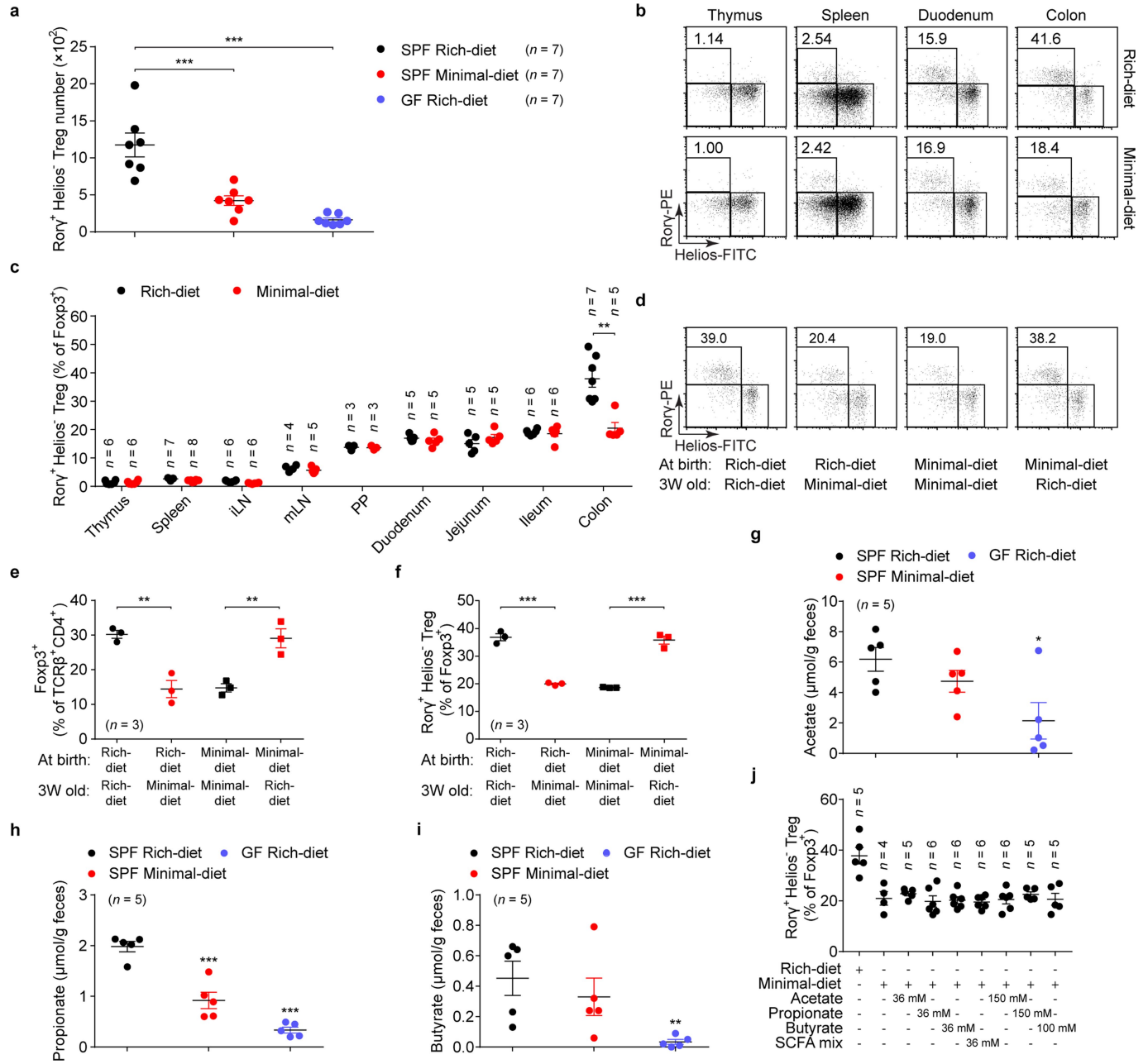

Extended Data Fig. 1 | Both dietary and microbial factors control the number of colonic RORγ$^+$T$_{reg}$ cells. a, Beginning at 3 weeks of age, three groups of mice were fed special diets for 4 weeks. SPF mice were fed either a nutrient-rich or a minimal diet, and GF mice were fed the nutrient-rich diet. Colonic T$_{reg}$ cells were analysed, and absolute numbers of RORγ$^+$Helios$^-$ in the FOXP3$^+$CD4$^+$TCRβ$^+$T$_{reg}$ cell population are shown. **b**, **c**, Three-week-old SPF mice were fed as in **a**, and T$_{reg}$ cells in different tissues were analysed after 4 weeks. Representative plots (**b**) and frequencies of RORγ$^+$Helios$^-$ in the FOXP3$^+$CD4$^+$TCRβ$^+$T$_{reg}$ cell population (**c**) are shown. iLN, inguinal lymph node. **d**–**f**, SPF mice were fed a nutrient-rich or a minimal diet at birth and were either maintained on that diet or switched to the opposite diet at 3 weeks of age. Colonic T$_{reg}$ cells were analysed after 4 weeks. Representative plots of RORγ$^+$Helios$^-$ in the FOXP3$^+$CD4$^+$TCRβ$^+$T$_{reg}$ cell population (**d**), and the frequencies of FOXP3$^+$ in the CD4$^+$TCRβ$^+$ cell population (**e**) and RORγ$^+$Helios$^-$ in the colonic FOXP3$^+$CD4$^+$TCRβ$^+$T$_{reg}$ cell population (**f**) are shown. **g**–**i**, LC–MS quantification of faecal acetate (**g**), propionate (**h**) and butyrate (**i**) from SPF mice fed a nutrient-rich or a minimal diet, and from GF mice fed a nutrient-rich diet. **j**, Three-week-old SPF mice were fed a nutrient-rich diet, a minimal diet, or a minimal diet supplemented with individual or mixed SCFAs in drinking water. Colonic T$_{reg}$ cells were analysed after 4 weeks. Frequencies of RORγ$^+$Helios$^-$ in the FOXP3$^+$CD4$^+$TCRβ$^+$T$_{reg}$ cell population are shown. Data are representative of two independent experiments. *n* represents biologically independent animals. Data are mean ± s.e.m. (**a**, **c** and **e**–**j**). $^*P < 0.05$, $^{**}P < 0.01$, $^{***}P < 0.001$, one-way ANOVA followed by the Bonferroni post hoc test (**a**, **e**–**i**) or two-tailed Student's *t*-test (**c**).

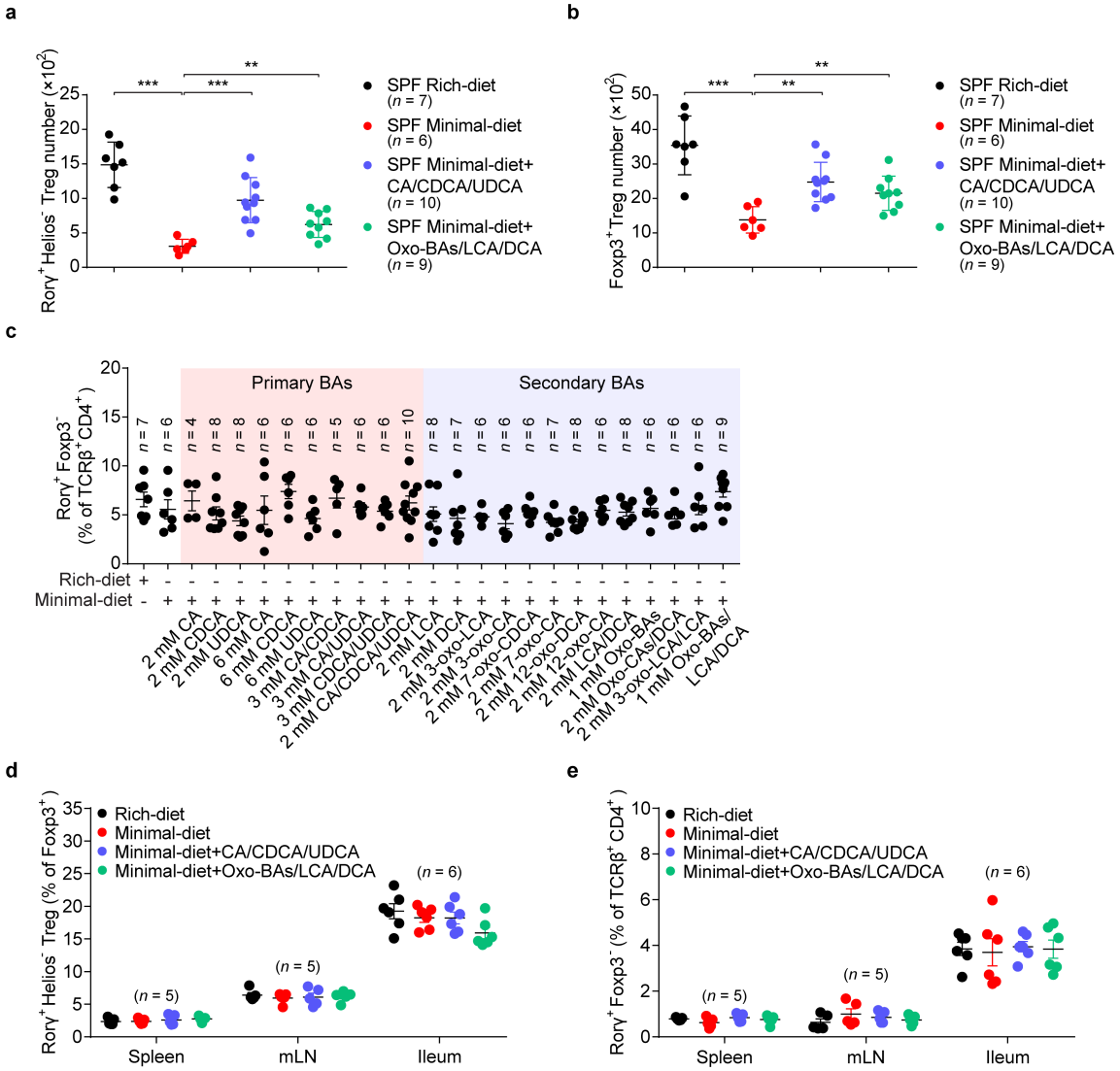

Extended Data Fig. 2 | Intestinal BAs regulate the number of colonic T_{reg} cells. a, **b**, Absolute numbers of RORγ$^+$Helios$^-$ in the colonic FOXP3$^+$CD4$^+$TCRβ$^+$ T_{reg} cell population (**a**) and of FOXP3$^+$ T_{reg} cells in the CD4$^+$TCRβ$^+$ population (**b**) in SPF mice fed a nutrient-rich diet, a minimal diet, or a minimal diet supplemented with mixtures of primary or secondary BAs in drinking water. The primary BAs were CA, CDCA and UDCA (2 mM of each). The secondary BAs were 3-oxo-CA, 3-oxo-LCA, 7-oxo-CA, 7-oxo-CDCA, 12-oxo-CA, 12-oxo-DCA, DCA and LCA (1 mM of each). **c**, Three-week-old SPF mice were fed a nutrient-rich diet, a minimal diet, or a minimal diet supplemented with one or more primary or secondary BAs in drinking water. Colonic T_H17 cells were analysed after 4 weeks. CA, CDCA, UDCA, DCA, LCA, 3-oxo-CA, 3-oxo-LCA, 7-oxo-CA, 7-oxo-CDCA, 12-oxo-CA, 12-oxo-DCA and the indicated BA combinations were tested. Frequencies of RORγ$^+$FOXP3$^-$ in the CD4$^+$TCRβ$^+$ cell population are shown. **d**, **e**, Three-week-old SPF mice were fed a nutrient-rich diet, a minimal diet, or a minimal diet supplemented with the indicated primary BAs (CA/CDCA/UDCA, 2 mM of each) or the secondary BAs (oxo-BAs/LCA/DCA, 1 mM of each) in drinking water. T_{reg} cells and T_H17 cells in the spleen, mesenteric lymph node and ileum were analysed after 4 weeks. Frequencies of RORγ$^+$Helios$^-$ in the FOXP3$^+$CD4$^+$TCRβ$^+$ T_{reg} cell population (**d**) and of RORγ$^+$FOXP3$^-$ in the CD4$^+$TCRβ$^+$ cell population (**e**) are shown. Data are pooled from two or three independent experiments. *n* represents biologically independent animals. Data are mean ± s.e.m. $^{**}P < 0.01$, $^{***}P < 0.001$, one-way ANOVA followed by the Bonferroni post hoc test.

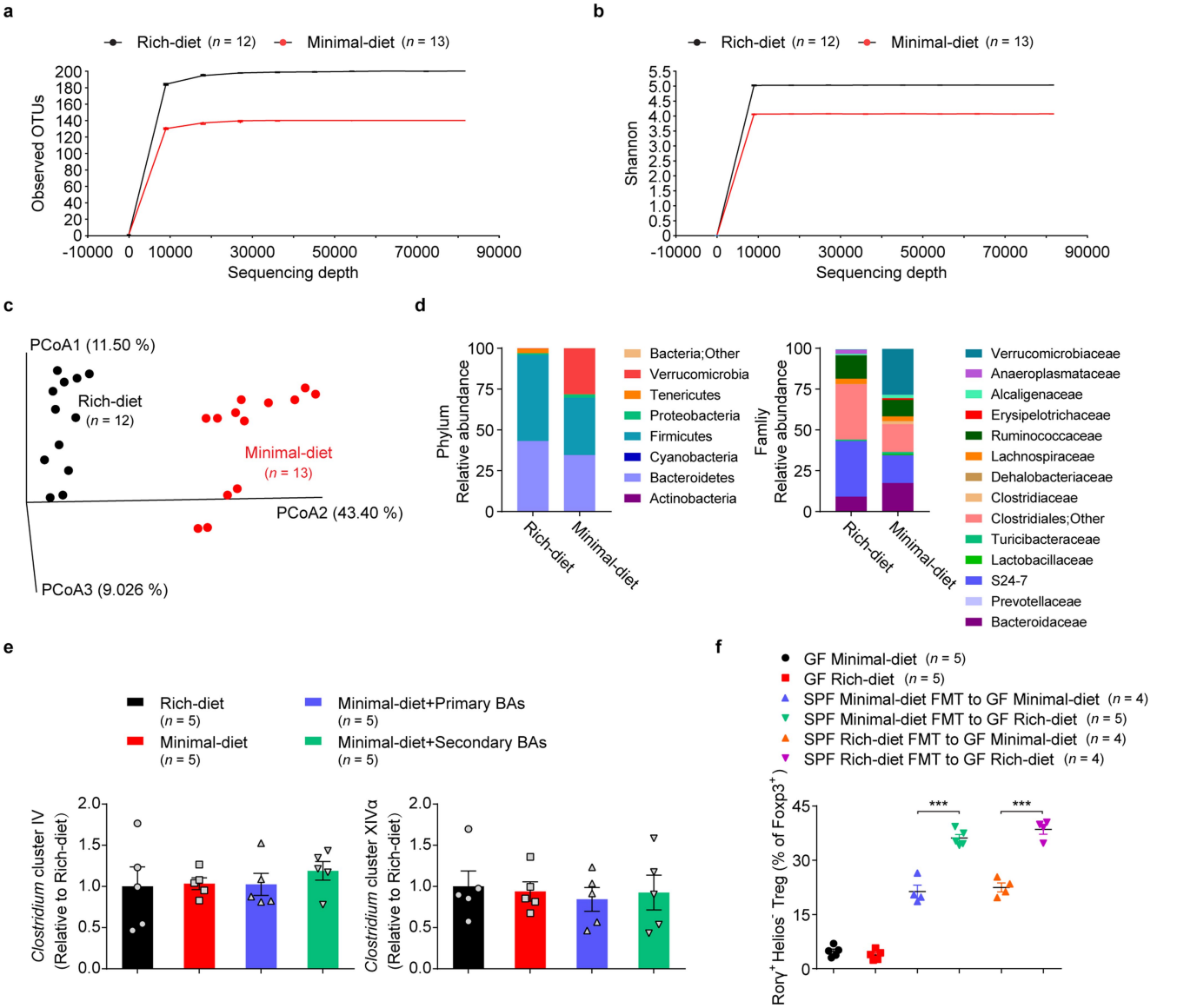

Extended Data Fig. 3 | Colonic microbial profiling of rich-diet mice versus minimal-diet mice. a–**d**, Three-week-old SPF mice were fed a nutrient-rich or a minimal diet, and the microbial compositions in the colonic lumen were analysed after 4 weeks by 16S rRNA sequencing. Observed operational taxonomic units (OTUs) (**a**), Shannon index (**b**), principal coordinates analysis (PCoA) (**c**) and the relative abundance of bacteria at the phylum and family levels (**d**) are shown. **e**, Quantitative PCR analysis of 16S rDNA of *Clostridium* cluster IV and *Clostridium* cluster XIVα in colonic luminal specimens from SPF mice fed a nutrient-rich diet, a minimal diet, or a minimal diet supplemented with the indicated primary BAs (CA/CDCA/UDCA, 2 mM of each) or the secondary BAs (oxo-BAs/LCA/DCA, 1 mM of each) in drinking water. **f**, Four-week-old GF mice or GF mice receiving transferred faecal materials (FMTs) from minimal-diet or rich-diet SPF mice were fed a nutrient-rich diet or a minimal diet, and colonic T_{reg} cells were analysed after 2 weeks. Frequencies of colonic RORγ$^+$Helios$^-$ in the FOXP3$^+$CD4$^+$TCRβ$^+$ T_{reg} cell population are shown. Data are pooled from three independent experiments in **a**–**d**. Data are representative of two independent experiments in **e** and **f**. *n* represents biologically independent animals. Data are mean ± s.e.m. ***$P < 0.001$, one-way ANOVA followed by the Bonferroni post hoc test.

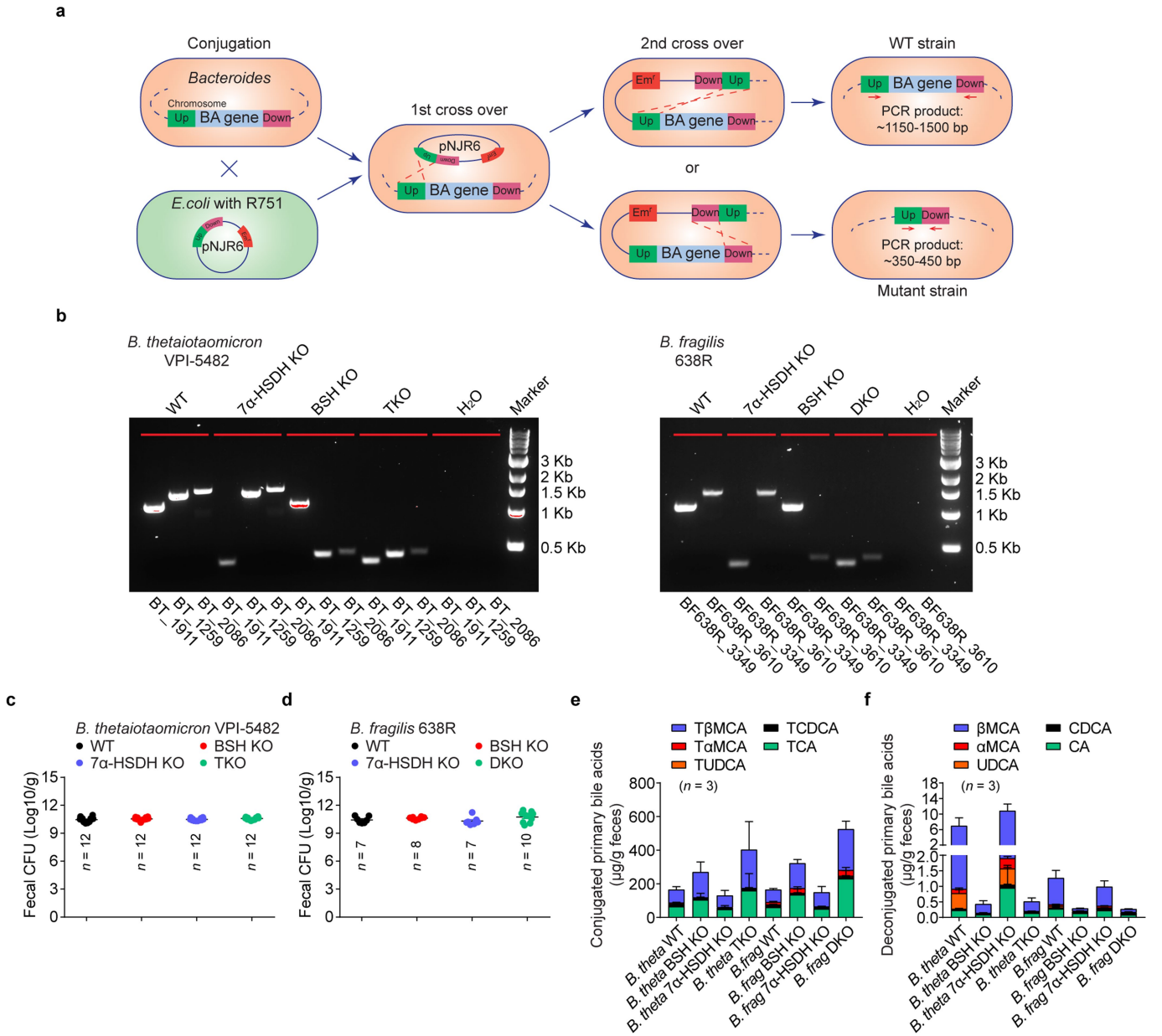

Extended Data Fig. 4 | Generation of BA metabolic pathway mutants in *Bacteroides*. **a**, Schematic diagram of pNJR6 suicide vector-mediated BA gene deletion in *Bacteroides*. **b**, Genotyping of *B. thetaiotaomicron* and *B. fragilis* BA metabolic pathway mutants by PCR. PCR primers were designed to target the flanking regions of an intact gene. PCR of an untouched gene plus its flanking regions generated a PCR product of around 1,150–1,500 bp, while deletion of an interested BA metabolic gene resulted in only an approximately 350–450-bp PCR amplicon of its two flanking regions. **c**, **d**, Bacterial load (measured as colony-forming unit (CFU) per gram of faeces) of *B. thetaiotaomicron* (**c**) and *B. fragilis* (**d**) BA metabolic pathway mutants and their wild-type control strains in monocolonized GF mice. **e**, **f**, LC–MS quantification of faecal conjugated primary BAs (**e**) and deconjugated primary BAs (**f**) in GF mice monocolonized with *B. thetaiotaomicron* or *B. fragilis* BA metabolic pathway mutants and their wild-type control strains. Data are representative of two independent experiments in **b**, **e** and **f**. Data are pooled from three independent experiments in **c** and **d**. *n* represents biologically independent animals. Data are mean ± s.e.m. (**c**–**f**).

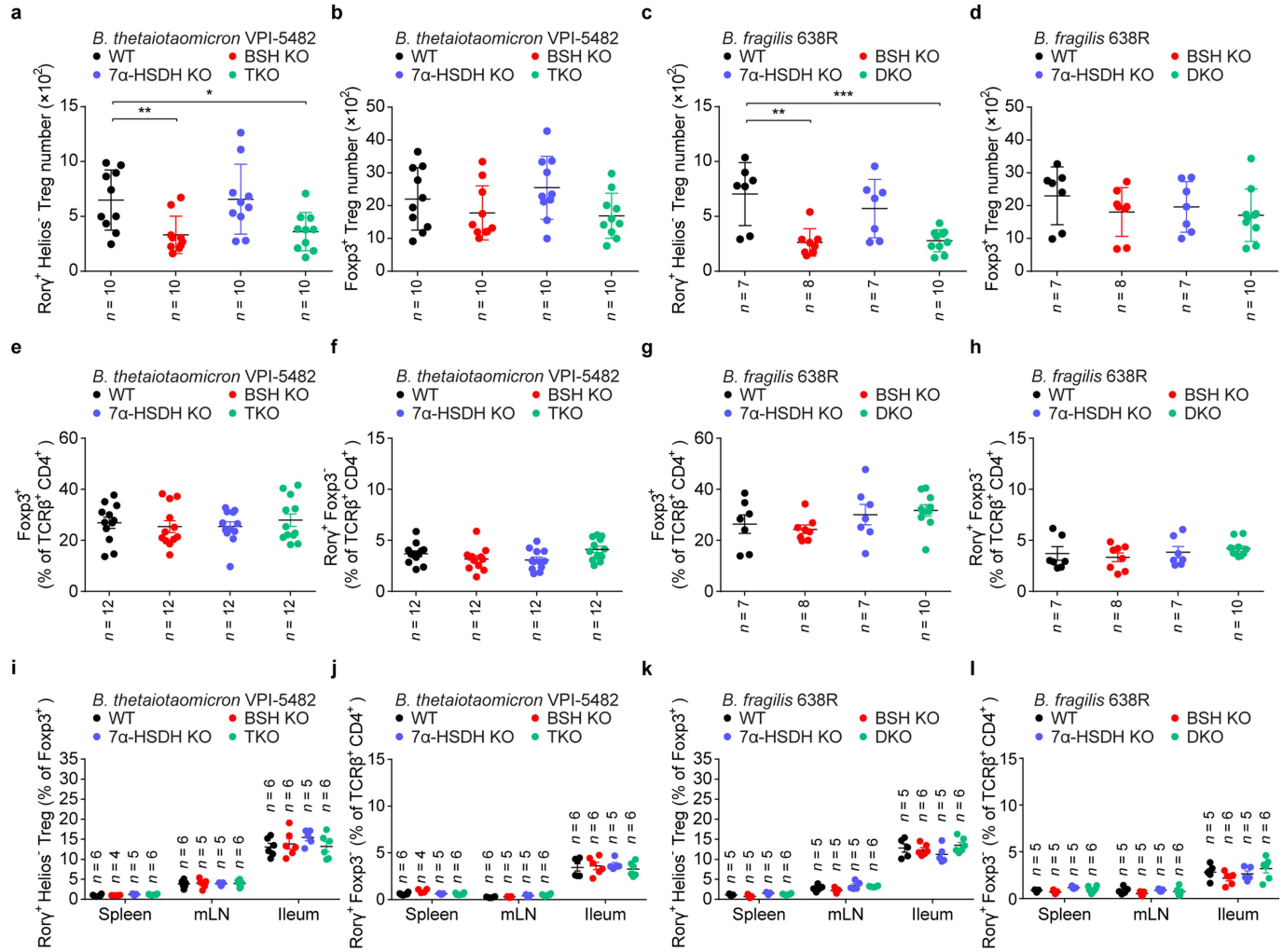

Extended Data Fig. 5 | Gut bacteria modulate colonic RORγ$^+$ T_{reg} cells via their BA metabolic pathways. a, **b**, Each of four groups of GF mice was colonized with one of the following microorganisms: (1) a wild-type strain of *B. thetaiotaomicron*; (2) a BSH-mutant strain; (3) a 7α-HSDH-mutant strain; or (4) a triple-mutant (TKO) strain. Colonic T_{reg} cells were analysed after 2 weeks. Absolute numbers of RORγ$^+$Helios$^-$ in the colonic FOXP3$^+$CD4$^+$TCRβ$^+$ T_{reg} cell population (**a**) and of FOXP3$^+$ T_{reg} cells in the CD4$^+$TCRβ$^+$ population (**b**) are shown. **c**, **d**, Each of four groups of GF mice was colonized with one of the following microorganisms: (1) a wild-type strain of *B. fragilis*; (2) a BSH-KO strain; (3) a 7α-HSDH-KO strain; or (4) a double-mutant (DKO) strain. Absolute numbers of colonic T_{reg} cells are shown as in **a** and **b**. **e**, **f**, GF mice were colonized with *B. thetaiotaomicron* BA metabolic pathway mutants or their wild-type control strains. Colonic T_{reg} cells and T_H17 cells were analysed after 2 weeks. Frequencies of FOXP3$^+$ in the CD4$^+$TCRβ$^+$ cell population (**e**) or RORγ$^+$FOXP3$^-$ in the CD4$^+$TCRβ$^+$ cell population (**f**) are shown. **g**, **h**, GF mice were colonized with *B. fragilis* BA metabolic pathway mutants or their wild-type control strains. Frequencies of colonic T_{reg} cells and T_H17 cells are shown as in **e** and **f**. **i**, **j**, GF mice were colonized with *B. thetaiotaomicron* BA metabolic pathway mutants or their wild-type control strains. T_{reg} cells and T_H17 cells in the spleen, mesenteric lymph node and ileum were analysed after 2 weeks. Frequencies of RORγ$^+$Helios$^-$ in the FOXP3$^+$CD4$^+$TCRβ$^+$ T_{reg} cell population (**i**) and RORγ$^+$FOXP3$^-$ in the CD4$^+$TCRβ$^+$ cell population (**j**) are shown. **k**, **l**, GF mice were colonized with *B. fragilis* BA metabolic pathway mutants or their wild-type control strains. Frequencies of T_{reg} cells and T_H17 cells in the spleen, mesenteric lymph node and ileum are shown as in **i** and **j**. Data are pooled from two or three independent experiments. *n* represents biologically independent animals. Data are mean ± s.e.m. $^*P < 0.05$, $^{**}P < 0.01$, $^{***}P < 0.001$, one-way ANOVA followed by the Bonferroni post hoc test.

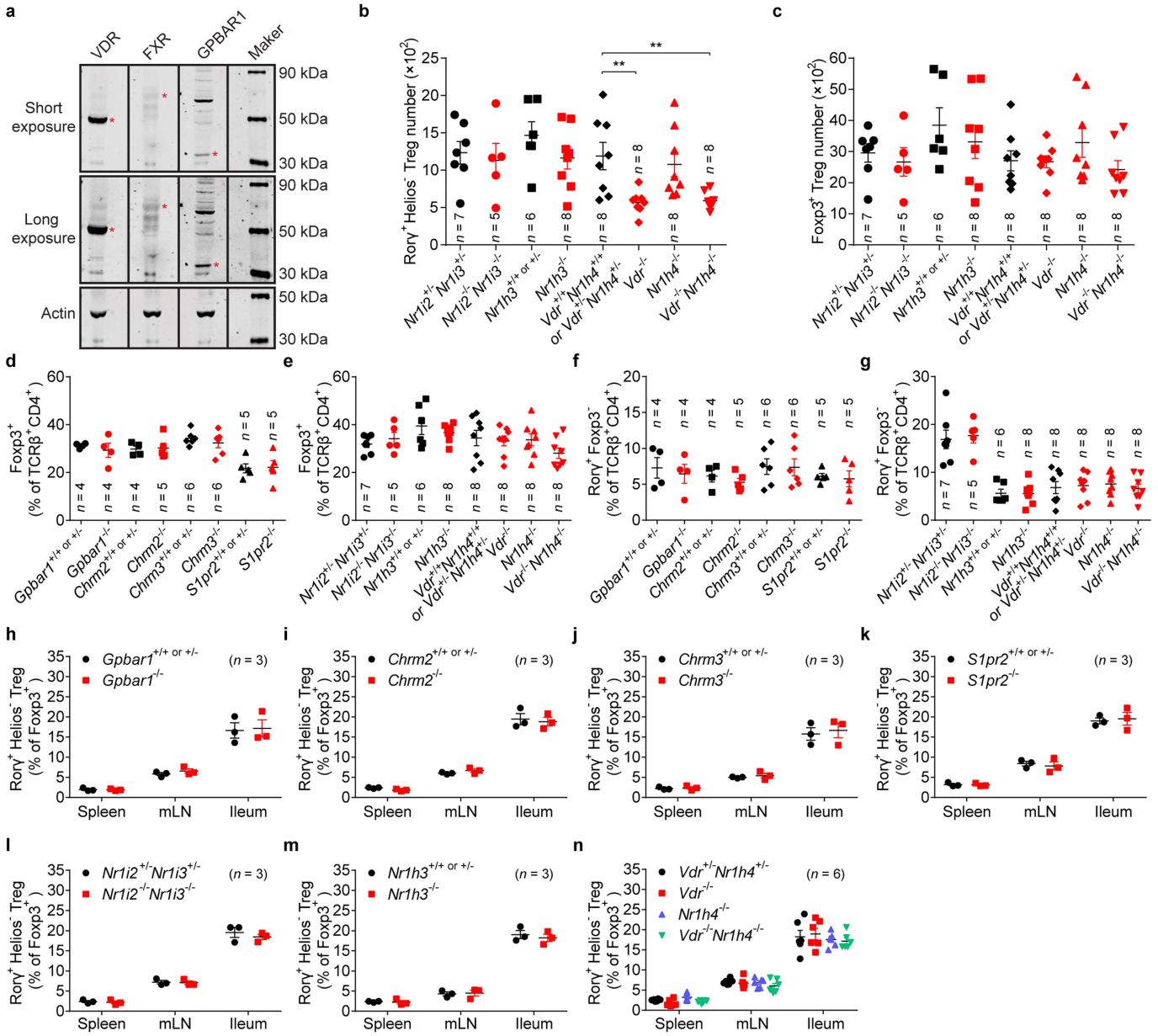

Extended Data Fig. 6 | The effect of BAR deficiency on T_{reg} cells or T_H17 cells in gut and peripheral lymphoid organs. a, Protein expression of VDR, FXR (also known as NR1H4) and GPBAR1 in the colonic tissue of SPF C57BL/6J mice was analysed by western blot. The red asterisks indicate the corresponding molecular weight of VDR (53 kDa), FXR (69 kDa) and GPBAR1 (33 kDa). For gel source data, see Supplementary Fig. 1. **b**, **c**, Absolute numbers of RORγ$^+$Helios$^-$ in the colonic FOXP3$^+$CD4$^+$TCRβ$^+$ T_{reg} cell population (**b**) and of FOXP3$^+$ T_{reg} cells in the CD4$^+$TCRβ$^+$ population (**c**) from mice deficient in nuclear receptors (*Nr1i2*$^{-/-}$*Nr1i3*$^{-/-}$, *Nr1h3*$^{-/-}$, *Vdr*$^{-/-}$, *Nr1h4*$^{-/-}$ and *Vdr*$^{-/-}$*Nr1h4*$^{-/-}$) and their littermate controls. **d**, **e**, Frequencies of FOXP3$^+$ in the colonic CD4$^+$TCRβ$^+$ cell population from mice deficient in G-protein-coupled receptors (*Gpbar1*$^{-/-}$, *Chrm2*$^{-/-}$, *Chrm3*$^{-/-}$ and *S1pr2*$^{-/-}$) and their littermate controls (**d**) and from mice deficient in nuclear receptors (*Nr1i2*$^{-/-}$*Nr1i3*$^{-/-}$, *Nr1h3*$^{-/-}$, *Vdr*$^{-/-}$, *Nr1h4*$^{-/-}$ and *Vdr*$^{-/-}$*Nr1h4*$^{-/-}$) and their littermate controls (**e**). **f**, **g**, Frequencies of RORγ$^+$FOXP3$^-$ in the colonic CD4$^+$TCRβ$^+$ cell population from mice described in **d** and **e**. **h**–**n**, T_{reg} cells in the spleen, mesenteric lymph node and ileum from the indicated mice were analysed. Frequencies of RORγ$^+$Helios$^-$ in the FOXP3$^+$CD4$^+$TCRβ$^+$ T_{reg} cell population from *Gpbar1*$^{-/-}$ (**h**), *Chrm2*$^{-/-}$ (**i**), *Chrm3*$^{-/-}$ (**j**), *S1pr2*$^{-/-}$ (**k**), *Nr1i2*$^{-/-}$*Nr1i3*$^{-/-}$ (**l**), *Nr1h3*$^{-/-}$ (**m**), and *Vdr*$^{-/-}$, *Nr1h4*$^{-/-}$ and *Vdr*$^{-/-}$*Nr1h4*$^{-/-}$ (**n**) mice and their littermate controls are shown. Data are representative of two or three independent experiments in **a** and **d**–**n**, or are pooled from two or three independent experiments in **b** and **c**. *n* represents biologically independent animals. Data are mean ± s.e.m. $^{**}P < 0.01$, one-way ANOVA followed by the Bonferroni post hoc test.

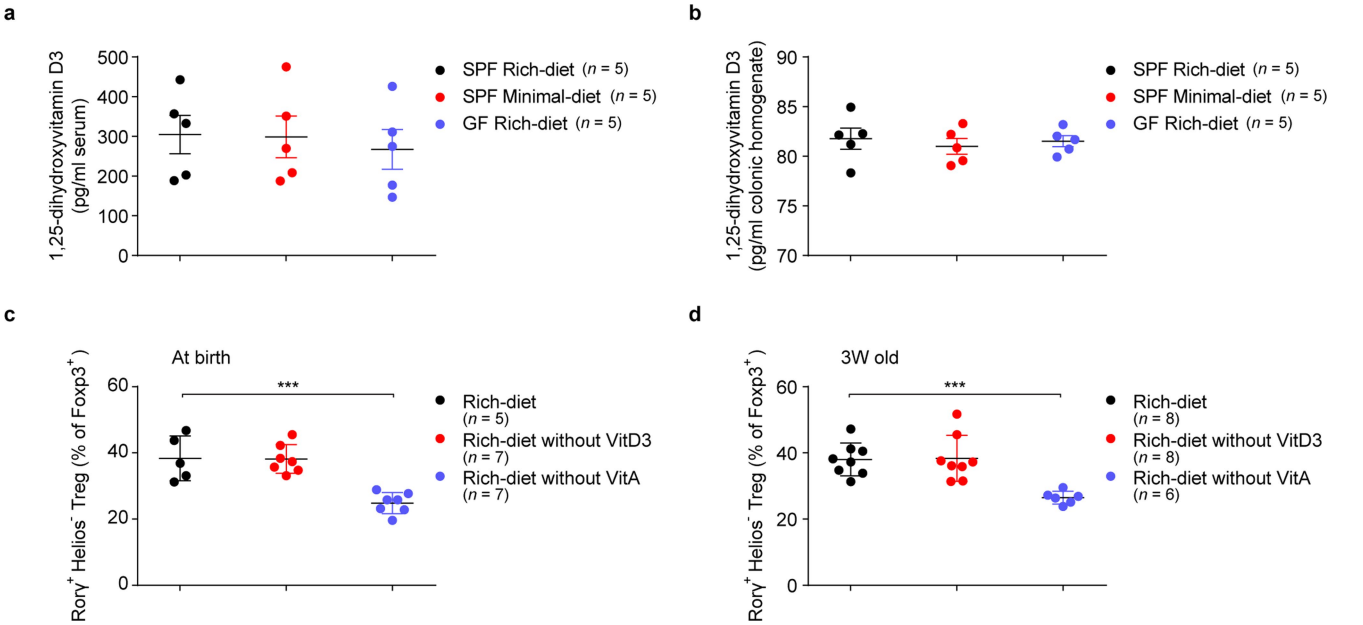

Extended Data Fig. 7 | Dietary vitamin D_3 does not alter the frequency of colonic RORγ$^+$ T_{reg} cells. a, **b**, Beginning at 3 weeks of age, three groups of mice were fed special diets for 4 weeks. SPF mice were fed either a nutrient-rich or a minimal diet, and GF mice were fed the nutrient-rich diet. The levels of 1,25-dihydroxyvitamin D_3 in serum (**a**) and the colon (**b**) of these mice were determined by ELISA. **c**, SPF mice were fed a nutrient-rich diet, or a rich diet deficient in vitamin D_3 (VitD3) or vitamin A (VitA) at birth. Colonic T_{reg} cells were analysed after 7 weeks. Frequencies of RORγ$^+$Helios$^-$ in the colonic FOXP3$^+$CD4$^+$TCRβ$^+$ T_{reg} cell population are shown. **d**, SPF mice were fed a nutrient-rich diet at birth and were either maintained on that diet or switched to a rich diet deficient in vitamin D_3 or vitamin A at 3 weeks of age. Colonic T_{reg} cells were analysed after 4 weeks. Frequencies of RORγ$^+$Helios$^-$ in the colonic FOXP3$^+$CD4$^+$TCRβ$^+$ T_{reg} cell population are shown. Data are representative of two independent experiments. *n* represents biologically independent animals. Data are mean ± s.e.m. ***$P < 0.001$, one-way ANOVA followed by the Bonferroni post hoc test.

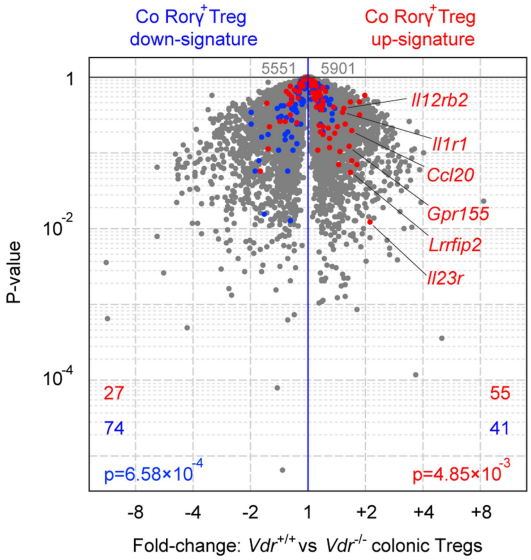

Extended Data Fig. 8 | Comparison of RORγ$^+$ T_{reg} cell signature genes of colonic T_{reg} cells from *Vdr*$^{+/+}$ and *Vdr*$^{-/-}$ mice. Volcano plots comparing transcriptomes of colonic T_{reg} cells from *Vdr*$^{+/+}$*Foxp3*^{mRFP} and *Vdr*$^{-/-}$*Foxp3*^{mRFP} mice ($n = 3$). Colonic RORγ$^+$ T_{reg} cell signature genes are highlighted in red (upregulated) or blue (downregulated). The number of genes from each signature preferentially expressed by one or the other population is shown at the bottom. Data are pooled from two independent experiments. *n* represents biologically independent animals. To determine the enrichment of certain gene signatures in RNA-seq datasets, a χ^2 test was used. $P < 0.05$ was considered statistically significant.

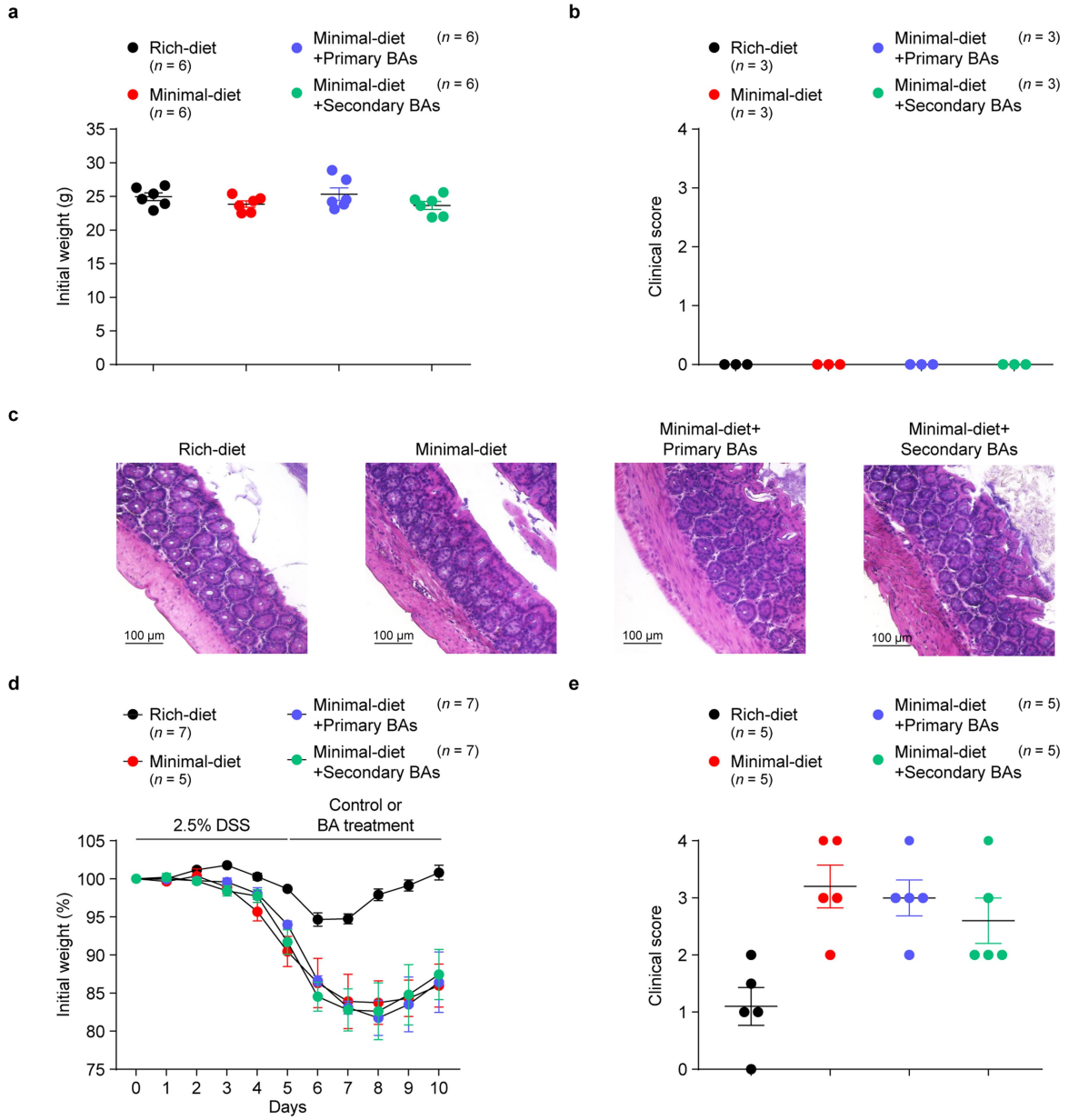

Extended Data Fig. 9 | BA supplementation does not cause gut inflammation and cannot ameliorate gut inflammation after the development of colitis. **a**–**c**, Three-week-old SPF mice were fed a nutrient-rich diet, a minimal diet, or a minimal diet supplemented with mixtures of primary BAs (CA/CDCA/UDCA, 2 mM of each) or secondary BAs (oxo-BAs/LCA/DCA, 1 mM of each) in drinking water. Initial body weights were recorded before DSS challenge (**a**). Clinical scores (**b**) and haematoxylin and eosin histology (**c**) for representative colons from mice not challenged with DSS are shown. **d**, **e**, Three-week-old SPF mice fed a nutrient-rich or a minimal diet for 4 weeks were then challenged in the DSS-induced colitis model. After the development of colitis at day 5 of the model, the DSS containing drinking water was switched to regular drinking water or to drinking water supplemented with mixtures of primary or secondary BAs. The primary BAs were CA, CDCA and UDCA (2 mM of each). The secondary BAs were 3-oxo-CA, 3-oxo-LCA, 7-oxo-CA, 7-oxo-CDCA, 12-oxo-CA, 12-oxo-DCA, DCA and LCA (1 mM of each). Daily weight loss (**d**) of mice during the course of DSS-induced colitis and clinical scores (**e**) on day 10 of colitis are shown. Data are representative of two independent experiments. *n* represents biologically independent animals. Data are mean ± s.e.m. in **a**, **b**, **d** and **e**.

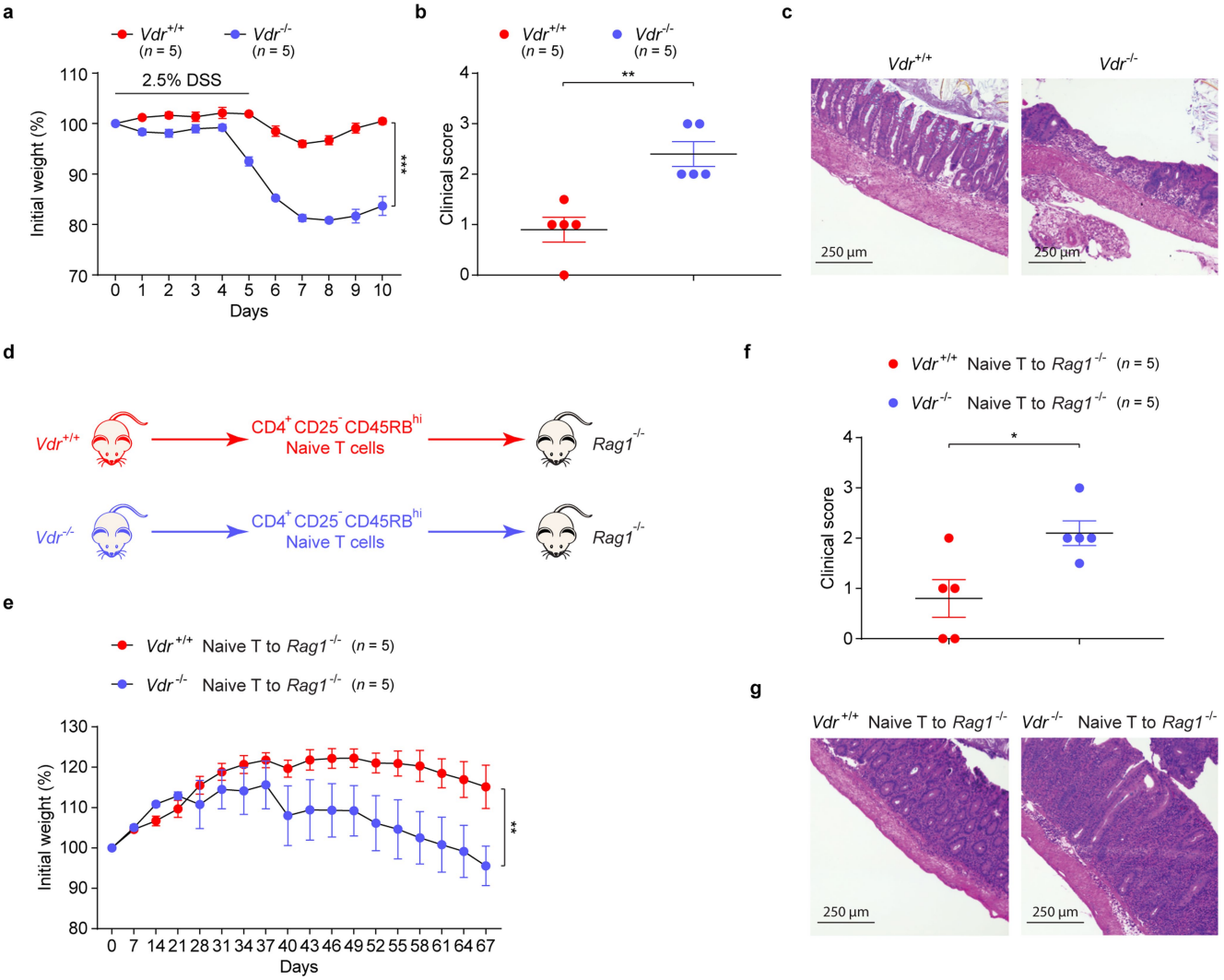

Extended Data Fig. 10 | VDR signalling controls gut inflammation. a–**c**, Daily weight loss (**a**) of *Vdr*$^{+/+}$ and *Vdr*$^{-/-}$ mice during the course of DSS-induced colitis. Clinical scores (**b**) and haematoxylin and eosin histology (**c**) of representative colons on day 10 of colitis are shown. **d**, Schematic representation of the T cell-adaptive transfer model of colitis. Either *Vdr*$^{+/+}$ or *Vdr*$^{-/-}$ naive T cells are transferred to *Rag1*$^{-/-}$ mice. **e**–**g**, Weight loss (**e**) of *Rag1*$^{-/-}$ mice in **d** during the course of T cell-adaptive transfer-induced colitis. Clinical scores (**f**) and haematoxylin and eosin histology (**g**) of representative colons on day 67 of colitis are shown. Data are representative of two independent experiments. *n* represents biologically independent animals. Data are mean ± s.e.m. in **a**, **b**, **e** and **f**. *$P < 0.05$, **$P < 0.01$, ***$P < 0.001$, two-way ANOVA followed by the Bonferroni post hoc test (**a** and **e**) or two-tailed Student's *t*-test (**b** and **f**).

nature research

Corresponding author(s): Dennis Kasper

Last updated by author(s): Oct 26, 2019

Reporting Summary

Nature Research wishes to improve the reproducibility of the work that we publish. This form provides structure for consistency and transparency in reporting. For further information on Nature Research policies, see Authors & Referees and the Editorial Policy Checklist.

Statistics

For all statistical analyses, confirm that the following items are present in the figure legend, table legend, main text, or Methods section.

n/a	Confirmed	
☐	☒	The exact sample size (*n*) for each experimental group/condition, given as a discrete number and unit of measurement
☐	☒	A statement on whether measurements were taken from distinct samples or whether the same sample was measured repeatedly
☐	☒	The statistical test(s) used AND whether they are one- or two-sided *Only common tests should be described solely by name; describe more complex techniques in the Methods section.*
☐	☒	A description of all covariates tested
☐	☒	A description of any assumptions or corrections, such as tests of normality and adjustment for multiple comparisons
☐	☒	A full description of the statistical parameters including central tendency (e.g. means) or other basic estimates (e.g. regression coefficient) AND variation (e.g. standard deviation) or associated estimates of uncertainty (e.g. confidence intervals)
☐	☒	For null hypothesis testing, the test statistic (e.g. *F*, *t*, *r*) with confidence intervals, effect sizes, degrees of freedom and *P* value noted *Give P values as exact values whenever suitable.*
☒	☐	For Bayesian analysis, information on the choice of priors and Markov chain Monte Carlo settings
☒	☐	For hierarchical and complex designs, identification of the appropriate level for tests and full reporting of outcomes
☒	☐	Estimates of effect sizes (e.g. Cohen's *d*, Pearson's *r*), indicating how they were calculated

Our web collection on statistics for biologists contains articles on many of the points above.

Software and code

Policy information about availability of computer code

Data collection	MACSQuantify™ Software was used to collect data from flow cytometry; Eppendorf MasterCycler was used to collect real-time PCR data; Thermo Scientific Orbitrap Q Exactive with Thermo Vanquish UPLC (UPLC-MS/MS) was used to collect MS data; Odyssey® CLx Fluorescence Imaging System was used to collect Immunoblot images; Zeiss Light Microscope was used to collect histological data; Illumina MiSeq was used to collect 16S rRNA profiling data; Illumina NextSeq500 was used to collect RNAseq data; BioTek® microplate reader was used to collect ELISA data.
Data analysis	Flow cytometric analyses were performed with the FlowJo 10.4.1; Thermo Xcalibur suite software version 3.0 was used to analysis the bile acid and SCFA data generated by UPLC-MS/MS (Thermo Scientific Orbitrap Q Exactive with Thermo Vanquish UPLC); 16S rRNA profiling data were analyzed by QIIME2; RNAseq data were analyzed by Cuffquant 2.2.1 and Multiplot Studio 1.5.60 in the GenePattern software package; ELISA data were obtained by BioTek® Gen5 software; Statistical analyses were performed with the GraphPad Prism 7.0 and Excel 2016.

For manuscripts utilizing custom algorithms or software that are central to the research but not yet described in published literature, software must be made available to editors/reviewers. We strongly encourage code deposition in a community repository (e.g. GitHub). See the Nature Research guidelines for submitting code & software for further information.

Data

Policy information about availability of data

All manuscripts must include a data availability statement. This statement should provide the following information, where applicable:

- Accession codes, unique identifiers, or web links for publicly available datasets
- A list of figures that have associated raw data
- A description of any restrictions on data availability

The authors declare that the data supporting the findings of this study are available within the paper and its supplementary information files. Accession codes will be available along with publication.

Field-specific reporting

Please select the one below that is the best fit for your research. If you are not sure, read the appropriate sections before making your selection.

☒ Life sciences ☐ Behavioural & social sciences ☐ Ecological, evolutionary & environmental sciences

For a reference copy of the document with all sections, see nature.com/documents/nr-reporting-summary-flat.pdf

Life sciences study design

All studies must disclose on these points even when the disclosure is negative.

Sample size	Sample sizes were based on a combination of the resource equation method, limited availability of gnotobiotic mice, and prior lab experience to ensure statistical and biological significance.
Data exclusions	No data was excluded from the analysis. Occasional growth restriction in mice fed a minimal diet (AIN-76A) necessitated their exclusion from all experiments. The exclusion criteria for growth restricted mice were pre-established.
Replication	Replicate experiments were preformed successfully at least two to three times. The number of replicates for each experiment is listed in the figure legends. If group size was small (due to limited availability of mouse strains), data from replicate experiments were pooled for graphical representation.
Randomization	Mice were randomized between groups when feasible. Age- and sex-matched littermates from each mouse line were bred as strict controls.
Blinding	Investigators were not blinded to the experimental groups given different housing conditions required. Clinical scores of hematoxylin/eosin stained colonic tissue sections were determined by a pathologist who was blinded to the nature of the mice under analysis.

Reporting for specific materials, systems and methods

We require information from authors about some types of materials, experimental systems and methods used in many studies. Here, indicate whether each material, system or method listed is relevant to your study. If you are not sure if a list item applies to your research, read the appropriate section before selecting a response.

Materials & experimental systems

n/a	Involved in the study
☐	☒ Antibodies
☒	☐ Eukaryotic cell lines
☒	☐ Palaeontology
☐	☒ Animals and other organisms
☒	☐ Human research participants
☒	☐ Clinical data

Methods

n/a	Involved in the study
☒	☐ ChIP-seq
☐	☒ Flow cytometry
☒	☐ MRI-based neuroimaging

Antibodies

Antibodies used	Following FACS antibodies were used in the study:PB-CD45 (30-F11, Biolegend, 103126), PE/Cy7-CD45 (30-F11, Biolegend, 103114), BV605-CD4 (GK1.5, Biolegend, 100451), PerCP/Cy5.5-CD4 (GK1.5, Biolegend, 100434), PE/Cy7-TCR-β (H57-597, Biolegend, 109222), FITC-TCR-β (H57-597, Biolegend, 109206), FITC-Helios (22F6, Biolegend, 137214), PE-RORγ (AFKJS-9, eBioscience™, 50-112-9700), APC-Foxp3 (FJK-16s, eBioscience™, 50-112-8936), APC/Cy7-Cd11c (N418, Biolegend, 117324), APC-CD8a (53-6.7, Biolegend, 100712), APC-CD19 (1D3/CD19, Biolegend, 152410), APC-F4/80 (BM8, Biolegend, 123116), APC-TER-119 (TER-119, Biolegend, 116212), PE-EpCAM (G8.8, Biolegend, 118206), PE-CD45RB (C363-16A, Biolegend, 103308), APC-CD25 (3C7, Biolegend, 101910), and anti-CD16/32 (2.4G2,BD Pharmingen™, 553142). Following WB antibodies were used in the study: Anti-VDR (sc-13133, Santa Cruz), Anti-FXR (sc-25309, Santa Cruz), Anti-GPBAR1 (PA5-23182, Invitrogen), Anti-Actin (sc-8432, Santa Cruz), IRDye® 680LT Goat anti-Rabbit IgG Secondary Antibody (P/N: 926-68021, LI-COR Biosciences), and IRDye® 680LT Goat anti-Mouse IgG Secondary Antibody (P/N: 926-68020, LI-COR Biosciences).
Validation	All the antibodies used in this study were validated by manufactures and used according to supplied instructions. The WB antibodies were re-validated by immunoblot performed in this study, and the FACS antibodies were determined by testing them with splenocyte staining.

Animals and other organisms

Policy information about studies involving animals; ARRIVE guidelines recommended for reporting animal research

Laboratory animals	C57BL/6J wild-type mice were obtained from Jackson, as were Vdr–/–, Nr1h4–/–, Nr1h3–/–, Chrm2–/–, Chrm3–/–, Rag1–/–, Foxp3YFP-cre, Cd11ccre, Vil1cre, and Foxp3mRFP mice. Nr1i2–/–Nr1i3–/– mice were obtained from Taconic. Gpbar1–/– mice were from KOMP Repository. S1pr2–/– mice were kindly provided by Dr. Timothy Hla at Boston Children's Hospital. Vdrflox/flox mice were kindly provided by Dr. David Gardner at University of California, San Francisco, and then crossed with Foxp3YFP-cre, Cd11ccre, or Vil1cre mice to generate the corresponding cell type specific knockout mice. Vdr–/–Nr1h4–/– mice were obtained by crossing Vdr+/– with Nr1h4+/– mice. Vdr–/–Foxp3mRFP or Vdr+/+Foxp3mRFP reporter mice were generated by crossing Vdr +/– with Foxp3mRFP reporter mice. All genetically modified mice and their control mice were subjected to experiments at the ages of 6-8 weeks old. For dietary treatment experiments, 3-week-old C57BL/6J wild-type mice or genetically deficient mice were fed either a sterilized nutrient-rich diet (LabDiet 5K67) or a minimal diet (TestDiet AIN-76A) for 4 weeks. Some groups of the mice fed a minimal diet were also treated with various BAs or SCFAs (sodium salt form) in drinking water for 4 weeks. GF C57BL/6J mice were orally inoculated by gavage with a broth-grown single bacterial strain or a collection of fecal material at 4 weeks of age. Each group of mice was then maintained in a gnotobiotic isolator under sterile conditions for 2 weeks.
Wild animals	The study did not involve wild animals.
Field-collected samples	The study did not involve samples collected from the field.
Ethics oversight	Harvard Medical School Institutional Animal Care and Use Committee and the Committee on Microbiological Safety.

Note that full information on the approval of the study protocol must also be provided in the manuscript.

Flow Cytometry

Plots

Confirm that:

☒ The axis labels state the marker and fluorochrome used (e.g. CD4-FITC).

☐ The axis scales are clearly visible. Include numbers along axes only for bottom left plot of group (a 'group' is an analysis of identical markers).

☐ All plots are contour plots with outliers or pseudocolor plots.

☒ A numerical value for number of cells or percentage (with statistics) is provided.

Methodology

Sample preparation	For isolation of LP lymphocytes, colonic and small intestinal tissues were dissected and fatty portions discarded. PPs were also removed from small intestines for isolation of lymphocytes. The excised intestinal tissues were washed in cold PBS buffer, and epithelia were removed by 500-rpm stirring at 37°C in RPMI medium containing 1 mM EDTA, 1 mM DTT, and 2% (vol/vol) FBS. After 15 min of incubation, the epithelium-containing supernatants were discarded, and the remaining intestinal tissues were washed in RPMI medium with 5% (vol/vol) FBS, further minced into small pieces, and digested by 500-rpm stirring at 37°C in RPMI medium containing collagenase type II (1.5 mg/ml), Dispase II (0.5 mg/ml), and 1.2% (vol/vol) FBS for 40 min. The digested tissues were filtered, and the solutions were centrifuged at 500 g for 10 min in order to collect LP cells. The pellets were resuspended, and the LP lymphocytes were isolated by Percoll (40%/80%) gradient centrifugation. For isolation of PP lymphocytes, the excised PPs were digested in the same medium by 500-rpm stirring at 37°C for 10 min, the digested PPs were filtered, the solutions were centrifuged at 500 g for 10 min, and lymphocytes were collected. Lymph nodes, spleens, and thymuses were mechanically disrupted.
Instrument	Miltenyi MACSQuant Analyzer and BD Biosciences MoFlo Astrios EQ.
Software	FlowJo 10.4.1.
Cell population abundance	All the cells were double sorted by flow cytometry (Astrios, BD Biosciences) to achieve 99% purity.
Gating strategy	The gating strategies used in this study: 1. FSC-A/SSC-A---FSC-A/FSC-H--- CD45-PB/Viability Dye-APC/Cy7---TCR-β-PE/Cy7/CD4-PerCP/Cy5.5---Foxp3-APC---RORγ-PE/ Helios-FITC. 2. FSC-A/SSC-A---FSC-A/FSC-H--- CD45-PE/Cy7/Viability Dye-DAPI---TCR-β-FITC/CD4-BV605---Foxp3-mRFP+/-. 3. FSC-A/SSC-A---FSC-A/FSC-H--- CD45-PE/Cy7/Viability Dye-DAPI---Cd11c-APC/Cy7. 4. FSC-A/SSC-A---FSC-A/FSC-H--- CD45-PB/Cy7-/Viability Dye-APC/Cy7---EpCAM-PE. 5. FSC-A/SSC-A---FSC-A/FSC-H--- CD45-PB/Viability Dye-AmCycan---TCR-β-PE/Cy7/CD4-PerCP/Cy5.5---CD25-APC-/CD45RB-PE high.

☐ Tick this box to confirm that a figure exemplifying the gating strategy is provided in the Supplementary Information.